Transactions of the American Fisheries Society 151:13–41, 2022

ISSN: 0002-8487 print / 1548-8659 online
DOI: 10.1002/tafs.10334

FEATURED PAPER

Capacity of Two Sierra Nevada Rivers for Reintroduction of Anadromous Salmonids: Insights from a High-Resolution View

David A. Boughton*
National Marine Fisheries Service, Southwest Fisheries Science Center, 110 McAllister Way, Santa Cruz, California 95060, USA

Lee R. Harrison
National Marine Fisheries Service, Southwest Fisheries Science Center, 110 McAllister Way, Santa Cruz, California 95060, USA; and Earth Research Institute, University of California, Santa Barbara, California 93106, USA

Sara N. John, Rosealea M. Bond, and Colin L. Nicol[1]
National Marine Fisheries Service, Southwest Fisheries Science Center, 110 McAllister Way, Santa Cruz, California 95060, USA; and Fisheries Collaborative Program, Institute of Marine Sciences, University of California Santa Cruz, 115 McAllister Way, Santa Cruz, California 95060, USA

Carl J. Legleiter
U.S. Geological Survey, Integrated Modeling and Prediction Division, Geomorphology and Sediment Transport Laboratory, 4620 Technology Drive, Golden, Colorado 80403, USA

Ryan T. Richardson
River Design Group, 236 Wisconsin Avenue, Whitefish, Montana 59937, USA

Abstract

Historically, anadromous steelhead *Oncorhynchus mykiss* and spring-run Chinook Salmon *O. tshawytscha* used high-elevation rivers in the Sierra Nevada of California but were extirpated in the 20th century by construction of impassable dams. Plans to reintroduce the fish by opening migratory passage across the dams and reservoirs can only succeed if upstream habitats have the capacity to support viable populations of each species. To estimate capacity in the Tuolumne and Merced rivers of the central Sierra Nevada, we used a high-resolution approach based on remote sensing and dynamic habitat modeling. Our results suggested that for both species in both systems, sediment grain sizes would support widespread spawning and the water temperatures, depths, and velocities would generate ample capacity for fry and juveniles. However, the unregulated Merced River was consistently too warm for adult Chinook Salmon to hold in the dry season prior to spawning, while the regulated Tuolumne River maintained a cooler, more stable thermal regime with a capacity for thousands of holding adults. In our high-resolution approach, we also discovered several specific physical controls on life history expression, including thermal constraints on the timing of spawning, hydraulic prompts for downstream migration of fry, divergence of the hydraulic niches of steelhead and Chinook Salmon, and a key but uncertain role for thermal tolerance in adult Chinook Salmon. Our results suggested

*Corresponding author: david.boughton@noaa.gov
[1]Present address: Ocean Associates, Inc., under contract to the National Marine Fisheries Service, Northwest Fisheries Science Center, 2725 Montlake Boulevard East, Seattle, Washington 98112, USA.
Received May 4, 2021; accepted September 22, 2021

that steelhead reintroduction could succeed in either system and Chinook Salmon could succeed in the Tuolumne River if passage strategies account for large numbers of migrant fry and juveniles driven downstream by winter storms and snowmelt. The Merced River appeared too warm for adult Chinook Salmon, which raises questions about the current limited understanding of thermal tolerance in holding adults. Our study shows how a high-resolution approach can provide valuable insights on specific limiting factors that must be addressed for reintroduction to succeed.

The Sierra Nevada mountains mark the eastern boundary of California's vast San Francisco Bay watershed, intercepting incoming Pacific storms and converting them to snowpack and a series of well-watered rivers draining westward through the Central Valley to the bay. Historically, most of the major rivers of the Sierra's western slope bore populations of steelhead *Oncorhynchus mykiss* (anadromous Rainbow Trout) and spring-run Chinook Salmon *O. tshawytscha*, which migrated up to high elevations to exploit cold mountain streams (McEwan 2001; Yoshiyama et al. 2001; Lindley et al. 2007). As elsewhere (Beechie et al. 2006; McClure et al. 2008), these high-elevation populations are now mostly gone or greatly diminished, victims of habitat destruction and 20th-century dam building that blocked migration (Yoshiyama et al. 2001) and threatened both runs with extinction (Williams et al. 2016). Lindley et al. (2007) determined that to reduce extinction risk in the watershed, new populations of steelhead and spring-run Chinook Salmon would need to be reintroduced into these high-elevation habitats. However, no such populations have been established since the two taxa were listed for protection under the U.S. Endangered Species Act two decades ago.

The San Joaquin River and its tributaries offer compelling options to re-establish anadromous steelhead and spring-run Chinook Salmon because these streams drain the highest elevations of the Sierra Nevada, where annual snowpack can sustain reliable and productive stream habitats (Yoshiyama et al. 2001), including into the future (Null et al. 2010). At the same time, the challenge of establishing fish passage around the dams (Lusardi and Moyle 2017) and improving migrant survival downstream of the dams (Perry et al. 2016; Buchanan et al. 2018) would require substantial investments for reintroduction to succeed. Obviously, the ultimate value of such investments depends on the current capacity of San Joaquin River tributaries to support viable or productive populations in their montane sections. For long-term viability, capacity would need to support an average of at least 2,500 spawners per tributary per generation, or about 600–800 spawners/year depending on the mean age at spawning (Lindley et al. 2007). Anecdotal accounts of spring-run Chinook Salmon from the 19th century suggest the potential for a much greater capacity—perhaps 200,000–500,000 spawners annually for the entire San Joaquin River system, or at the very least "great hordes" whose "leaping over the sandbars created a noise comparable to a large waterfall" (Yoshiyama et al. 2001:90 and references cited therein). Such capacity could support a valuable fisheries resource, but the current capacities of San Joaquin River tributaries are not known.

Productive capacity, or carrying capacity, is broadly defined as the number of organisms of a given species that can be supported by a given area of habitat (Sayre 2008). For habitat that is currently vacant or underused, capacity is commonly inferred from specific factors thought to limit population growth (Sayre 2008). Key challenges of this inductive approach are that capacity typically fluctuates in time and varies in space (McLeod 1997; del Monte-Luna et al. 2004; Sayre 2008; Chapman and Byron 2018) and that different species and environmental settings are subject to a great diversity of limiting factors and mechanisms for density dependence (e.g., McLeod 1997; Braithwaite et al. 2012; O'Neil et al. 2014; Steenweg et al. 2016; Cooper et al. 2020; Taylor et al. 2020), which impedes a unified approach across taxa and habitats (McLeod 1997; Sayre 2008).

Inductive approaches generally sort into two general concepts: actual capacity under current conditions versus the intrinsic or maximum potential capacity under optimal conditions (Leopold 1933; Sayre 2008). For California salmonids, intrinsic potential has been inferred from static spatial data on elevation, climate, and geology, with mean fish abundance in pristine reference watersheds used to calibrate the estimates (Agrawal et al. 2005; Bjorkstedt et al. 2005; Burnett et al. 2007). Actual capacity has been inferred for a few watersheds in California using coupled coarse-resolution habitat and salmon population models (Stillwater Sciences 2012). Although these tools provided valuable insight at the watershed scale, they had their limits. Their coarse spatial and temporal resolution did not match the finer scale at which density-dependent mechanisms of movement and competition typically unfold during spawning by adults (Falcy 2015; Huntsman et al. 2017; Bouchard et al. 2018) or rearing by juveniles (Chapman 1966; Grant and Kramer 1990; Ayllon et al. 2012; Rosenfeld 2014). Thus, they could not predict variability through time, such as under variable hydrology or climate change. This provided little insight into the operation of specific limiting factors or how those factors might respond to various natural and anthropogenic forcing mechanisms.

More could be learned by estimating capacity at higher spatial and temporal resolution to capture habitat dynamics at the scale of a key mechanism: fish competing for space (Ayllon et al. 2012). At the same time, to evaluate reintroduction the spatial and temporal extents of the estimates need to cover entire populations over multiple generations (Williams 1996, 2010; Railsback 2016). Unlike inductive estimates of capacity for most animal species (Sayre 2008), for salmonids a high-resolution approach has been validated empirically. Ayllon et al. (2012) successfully estimated and validated time series of capacity for Brown Trout *Salmo trutta* as a function of cover, water depth, and water velocity at meter-scale resolution. Although they only quantified a specific point in each year's low-flow season and spatial extent only covered individual reaches, their capacity estimates explained 39–56% of annual fluctuations in the density of various life stages of Brown Trout over 12 years, with much of the remaining variation explained by demography, interstage competition for space, and water temperature. Their limited spatial extent mostly stemmed from the practical rigors of mapping channel bathymetry at high resolution, but recent advances in remote sensing of rivers have relaxed this limit, opening a truly "riverscape" approach (Fausch et al. 2002; Carbonneau et al. 2012). For example, red and green airborne LiDAR and multispectral and hyperspectral imaging (Legleiter et al. 2009; Passalacqua et al. 2015; Hugue et al. 2016; Tonina et al. 2019) are all now used to construct meter-resolution digital elevation models (DEMs) of the river channel and floodplain, suitable for hydraulic modeling of instream habitat (Legleiter 2012). By combining process-based models of flow hydraulics (Wilkins and Snyder 2011; Benjankar et al. 2018), coarse-sediment dynamics (Buffington et al. 2004; Pfeiffer and Finnegan 2017), and thermal patterns (Pike et al. 2013), the physical predictors of habitat use by salmonids can be quantified in high spatial and temporal resolution at the riverscape scale (McHugh et al. 2017; Wheaton et al. 2018).

Here, we use this high-resolution, broad-extent approach to ask the following: What is the capacity for reintroduction of steelhead and spring-run Chinook Salmon to two San Joaquin River tributaries, the Merced and Tuolumne River systems? Specifically, how do estimates of capacity compare to criteria for viable populations in each river system, and looking beyond viability, do they suggest the capacity for creation of a productive resource? In pursuing these questions using a high-resolution approach, we also found several specific ways in which physical forcing mechanisms constrain the expression of life history and thus the prospects for reintroduction. These include constraints on the timing of spawning, prompts for the downstream migration of fry, divergence of the hydraulic niches of steelhead and Chinook Salmon, and a key but uncertain role for thermal tolerance in adult Chinook Salmon. The modular workflow that we describe is flexible and adaptable to a variety of questions involving the introduction of fish into vacant habitat.

METHODS

Species life history.— For our species, the overall carrying capacity of each population involves a sequence of life stages, each with its own specific habitat associations, density-independent survival, and capacity (Mobrand et al. 1997; Greene and Beechie 2004). All of the stage-specific survivals and capacities in montane, lowland, and marine habitats must ultimately be estimated to determine overall productivity and population viability, but this larger question is outside the scope of our study. Instead, as a first step to determining the feasibility of reintroduction, we focused on estimating capacity for the subset of life stages that would use the montane portion of each river system: spawning pairs of adults (estimated as redd capacity), fry (FL < 60 mm), juveniles (FL > 60 mm), and for Chinook Salmon only, adults that hold in pools prior to spawning.

Life history plays out within the distinctive Mediterranean-type flow regime of California rivers, where most precipitation falls from October to April. During the wet season, river discharge spikes after storms at the lower, warmer elevations, with a broader peak emerging in May or June from snowmelt at higher elevations. May–September is the dry season, and once the snowpack has melted—typically sometime in July—river discharges decline steadily until the first big storms of October or November.

Within this hydraulic template, the two species time their life stages differently (Table 1). Adults of spring-run Chinook Salmon migrate up to high elevations on the spring snowmelt and hold in pools through the dry season until spawning in the fall (Garman and McReynolds 2009). Eggs incubate in gravel nests (redds), and the resulting fry disperse from the redds mid-winter and establish home ranges that expand as they grow into the juvenile size range (Grant and Kramer 1990). Juveniles pursue one of two life histories: a subyearling form that migrates down to valley or estuarine habitats by the end of the wet season; and a rarer yearling form that stays for the dry season and migrates after the rains resume the following fall (Garman and McReynolds 2009). Analysis of adult otoliths from some remaining populations in the northern Sierra Nevada shows that despite the rarity of the yearling form, it contributes disproportionately to adult runs, especially during drought years when harsh conditions at lower elevations select against the subyearling form (Cordoleani et al. 2021). Here, we explicitly consider capacity for both forms.

TABLE 1. Seasonality of Chinook Salmon and steelhead life stages used in modeling.

Life stage	Description	Months present[a]											
		Jan	Feb	Mar	Apr	May	Jun	Jul	Aug	Sep	Oct	Nov	Dec
Spring-run Chinook Salmon[b]													
Adult holding	From migration to spawning		<	<	<	P	P	P	P	P	>		
Spawning	Construction of redds									P	P		
Incubation	Eggs to emergence of fry	>	>							P	P	P	P
Fry rearing	Rearing of fish <60 mm FL	P	P	>								<	P
Juvenile rearing	Rearing of fish >60 mm FL		s	s	s	s	d	d	d	d	f	f	f
Steelhead[c]													
Spawning	Construction of redds	P	P	P	P	>	>				<	<	P
Incubation	Eggs to emergence of fry	P	P	P	P	P	P	>	>		<	<	P
Fry rearing	Rearing of fish <60 mm FL	<	<	P	P	P	P	P	P	P	>	>	
Juvenile rearing	Rearing of fish >60 mm FL	w	w	w	s	s	s	d	d	d	f	f	f

[a]P = peak season; < = early season; > = late season. For juveniles, s = spring season; d = summer (dry) season; f = fall season; and w = winter season.

[b] From accounts of Central Valley populations by Yoshiyama et al. (1998) and Garman and McReynolds (2009). Subyearling and yearling juveniles are present in the spring season; yearlings continue freshwater occupancy through the dry season and the fall season.

[c]From accounts of Central Valley populations by McEwan (2001).

In contrast to Chinook Salmon, adult steelhead spawn throughout the entire wet season (Table 1). As a result, fry may be seen for much of the year, though tending to peak in the dry season (McEwan 2001). Juveniles stay in freshwater for one or more complete years before migrating down to the ocean, typically toward the end of the wet season in April or May. Historically, the return migration of adult steelhead in Central Valley streams occurred over a broad window—in the last century, adults were observed migrating in every week of the year within the Sacramento River, although the greatest abundance by far was a fall run from August through October (McEwan 2001). Prior to the construction of large dams, a spring or summer run may have been more prevalent (Needham et al. 1941; Lee 2020), adopting a prespawn holding strategy similar to that of spring-run Chinook Salmon. Evidence for large spring or summer runs is sparse, especially in the San Joaquin River drainage. More recently, Central Valley steelhead have been observed to mostly migrate in the winter concurrent with the spawning season (Busby et al. 1996; McEwan 2001; Stanley et al. 2020). Here, we assume a winter run, but we note that a fall or spring run could potentially emerge under appropriate environmental conditions if alleles for an earlier, pre-maturation run timing (McEwan 2001) are still extant in wild populations (Kannry et al. 2020).

Conceptual approach.— Over the typical season for each life stage of each species, we modeled daily carrying capacity as a dynamic function of physical habitat:

$$K(t)_j = D_j \sum_i A(t)_i P(\mathbf{x}_{t,i})_j, \quad (1)$$

where $K(t)_j$ = capacity (number of fish) of a given river segment for life stage j at time t; D_j = density at capacity (fish/m^2) of life stage j in suitable habitat, assumed constant; $A(t)_i$ = area (m^2) of a small spatial element i of river channel at time t; $P(\mathbf{x}_{t,i})_j$ = incidence at capacity (probability of occupancy) for life stage j in habitat element i; and the summation covers the spatial extent of habitat that is accessible to the fish.

Here, density at capacity and incidence at capacity were theoretical constructs for fully saturated habitat in the sense that any extra fish would emigrate or die (Greene and Beechie 2004). A daily time step is appropriate since it captures the relevant temporal scale of key density-dependent demographic processes, such as density-dependent mortality in fry and especially dispersal in juveniles (Einum et al. 2006). Incidence at capacity, $P(\mathbf{x}_{t,i})_j$, was treated as a function of a time-varying vector of three physical traits of rivers: water depth, vertically averaged water velocity, and temperature. Physical traits were inferred using a series of physics-based and regression models, with the size of each small spatial element i (typically 1 m^2) determined by the resolution of an underlying DEM. The DEM represented the channel bed and was generated by remotely sensing the rivers. For spawning capacity, we modeled a fourth physical factor—the median grain size of sediment in the channel bed—because spawning capacity is tightly linked to the fraction of grains that are small enough to be moved by spawning adults (Riebe et al. 2014). Equation (1) assembled these parts into a modular structure, in which each part could be constructed separately using methods appropriate to the available information and computing power.

Other factors influencing capacity, such as cover, prey, and predators, were treated implicitly by estimating $P(\mathbf{x}_{t,i})_j$ using data from river systems that could serve as ecological

analogs. Ecological analogs can be identified as sites with similar biotic and abiotic traits as the reintroduction site and where the focal species had a similar phenotype and local adaptation as the reintroduction stock (Perkins and Leffler 2018). In practice, this implicit treatment of some factors implied that the peak of the incidence function (P_{max}) could fall below 1.0 because even if the explicit factors were optimal, the implicit factors might limit incidence.

Similarly, density at capacity may depend on implicit factors, such as cover and prey (Grant and Kramer 1990; Imre et al. 2004), which we dealt with by using data from ecological analogs. By treating density as constant, we assumed that the incidence function explained variation in density at coarser scales, such as among pools, glides, and riffles. Although such variation is often observed, it is typically attributed to differing availability of preferred depths and velocities (e.g., Nickelson et al. 1992), supporting our assumption.

Spatial and temporal extent.— The Merced and Tuolumne rivers rise in Yosemite National Park at 4,000-m elevation and flow west about 240 km to join the San Joaquin River in the Central Valley. We focused our remote sensing on their montane sections above two large reservoirs (Figure 1) but below second-order limits to anadromy reported upstream of these reservoirs by Yoshiyama et al. (2001). We examined 57 km of the Merced River and the South Fork Merced River and 52 km of the Tuolumne River and its tributary, Cherry Creek (Figure 1; see also Table S.1 available in the Supplement in the online version of this article). Another tributary, the Clavey River, was imaged but lacked sufficient discharge data to estimate capacity. Both river systems are protected as Wild and Scenic Rivers, but only the Merced River had a natural flow regime. The Tuolumne River and Cherry Creek were regulated by upstream dams and a series of hydropower stations with tunnels and outflows (Hanson et al. 2005).

For temporal extent, we estimated daily capacity across 10 years to cover about three generations of each species (most adults spawn at age 3 or 4). We chose the years 2008–2017 based on available temperature data and to capture recent conditions. Annual rainfall and stream discharge in the western USA are typically quantified for the "water year" (WY) running from October of the previous year through September of the current year so as to lump all runoff from a given wet season. According to the Pohono Bridge gauge on the Merced River (U.S. Geological Survey station 11266500), our temporal extent included the highest annual discharge on record (WY 2017) and the second-lowest annual discharge (WY 2015). We used these years to learn how capacity responded to extremes in precipitation. The Pohono Bridge gauge is near the lower end of Yosemite Valley and represents a completely natural flow regime over a 102-year period of record.

Channel bathymetry.— Channel bathymetries with 1-m resolution were constructed using red LiDAR for the exposed part of the channel and hyperspectral imagery for the submerged portion (see Figure S.1 [available in the Supplement in the online version of this article] for examples; remote sensing details are provided in the methodological notes of the Supplement). Although green LiDAR can penetrate water and generate bathymetry, we would need a helicopter to acquire it in our narrow canyons, and this was too expensive.

Under the hyperspectral approach, we predicted water depths from the band ratio

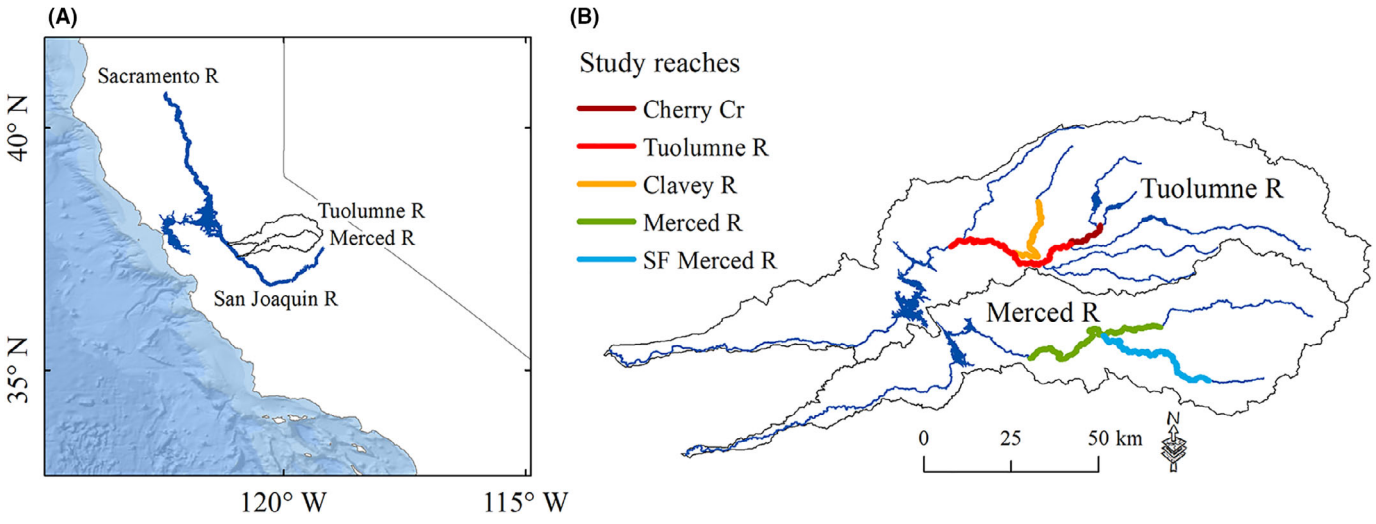

FIGURE 1. Location map showing **(A)** the Merced and Tuolumne River watersheds in California and **(B)** five reaches for which data were remotely sensed (SF = South Fork).

$$X = \ln\left[\frac{R(\lambda_1)}{R(\lambda_2)}\right] \quad (2)$$

(Legleiter et al. 2009), where $R(\lambda_1)$ and $R(\lambda_2)$ are the reflectance values for 2 of the 48 spectral bands (colors) in the hyperspectral imagery. Concurrent to remote sensing, we also sampled water depths (d) in the stream itself, with highly accurate coordinates so that we could pair them with individual pixels in the imagery. We then used linear regression to relate d to X for these pixels and to predict d from X for the remaining pixels across the full extent of the remotely sensed channel. The resulting depth maps were then aligned to the LiDAR topography, and the reconstructed depths were subtracted from the water surface elevation in the LiDAR DEM to create a continuous bathymetric–topographic surface for the entire stream corridor.

We sampled d near Lumsden Campground on the Tuolumne River and west of Briceburg on the Merced River; these were accessible sites with a variety of water depths dispersed among pools and riffles. To sample d, we used a real-time kinematic GPS to obtain water surface elevation from the edge of the wetted channel and bed elevation from wadable areas. We subtracted each bed elevation from the nearest water surface elevation to obtain d. For nonwadable areas, we sampled d from a kayak equipped with an integrated real-time kinematic GPS and survey-grade echo sounder. The echo sounder's reported accuracy was 0.01 m, and its operating range was 0.3–75.0 m.

To construct X, we first had to select two spectral bands, λ_1 and λ_2, from the 48 bands of the hyperspectral images. To select λ_1 and λ_2, we used optimal band ratio analysis (Legleiter et al. 2009), in which the field data for d are regressed on X for each possible band pair (1,128 total), and the pair with the highest R^2 is chosen. We randomly selected half of the field data to fit the regressions and the rest of the data to test accuracy. We included a quadratic term (X^2) to improve depth retrieval in deeper pools. The Merced River optimal band ratio analysis was also presented in a master's thesis by Richardson (2016).

Water depths and velocities.— Each river's DEM was input to a hydraulic model to predict 10 years of daily water depth and velocity at 1-m^2 resolution. Ideally, such predictions would come from a fully calibrated two-dimensional (2D) unsteady-flow model. This ideal was well beyond our computational resources, so we made a number of simplifying assumptions (similar to Harrison et al. 2017). Rather than model unsteady flow, we modeled steady flow at each of 34 "design flows" ranging from 0.03 to 396.5 m^3/s, which spanned the historical range. A library of capacity estimates (see below) was then constructed for each design flow and used to linearly interpolate capacity at other discharges representing the unsteady flow pattern from 2008 to 2017. Rather than apply a 2D flow model, which resolves spatial patterns of depth and velocity both longitudinally and laterally within the channel, we applied a one-dimensional model using the Hydrologic Engineering Center River Analysis System (HEC-RAS), which only resolves the longitudinal pattern and at less than the desired spatial resolution. We then interpolated "quasi-2D" depth and velocity maps at high resolution for each design flow. These simplifying assumptions omit transient effects during storms or dam releases and do not capture the full complexity of a 2D flow field, such as lateral water movements in meander bends and boulder fields.

The HEC-RAS is a widely used hydraulic model that employs an implicit finite-difference scheme to solve equations for the conservation of mass and momentum (USACE 2016). The model predicts the water surface elevation and mean velocity at each channel cross section it receives as input. We derived the cross sections from the channel DEMs, spacing them tightly (mean spacing = 15 m) to produce a comprehensive library of mean depths and velocities (n = 4,056 cross sections in the Merced River system; 5,415 cross sections in the Tuolumne River system). The quasi-2D flow fields were then computed using the HEC-RAS Mapper by (1) interpolating water surface elevation at 1-m^2 resolution between adjacent cross sections; (2) calculating depth from the difference between water surface and DEM surface; and (3) estimating vertically averaged water velocity from the depths using Manning's equation and a normalization scheme (Brunner 2010).

For each river system, the hydrograph of actual unsteady flows from 2008 to 2017 was reconstructed from gauge data. Daily flow measured at gauges was assumed to extend upstream and downstream to major tributaries; contributions of tributaries were subtracted or added to extend flow estimates further upstream or downstream, respectively (see Table S.2 for gauge metadata and notes). We could not reconstruct WY 2008 in the Tuolumne River system due to missing data; we filled other smaller gaps in the discharge record using singular-spectrum analysis (Golyandina and Korobeynikov 2014). To capture effects of sub-daily changes in discharge, separate hydrographs were made for the daily mean, maximum, and minimum discharge. We then interpolated daily capacity for each of the three hydrographs from the library of design flows, and we assumed that the smallest of the three values for each day represented actual capacity.

Grain sizes.— To quantify channel substrate, we estimated the median grain size (diameter D_{50}) expected at each channel cross section. Our estimates used the concept of competent D_{50} (Buffington et al. 2004)—the grain size for which the boundary shear stress imposed on the grain by streamflow at bank full was just enough (competent) to mobilize the grain (Buffington et al. 2004; Wilkins and Snyder 2011; Pfeiffer and Finnegan 2017). Thus, it predicted the divide between grains that were just small enough to be mobilized and those that were just large

enough to accumulate on the streambed. The proportion of total shear stress available to transport sediment was empirically calibrated for each system using field observations of D_{50}. We adapted the stress-partitioning method of Pfeiffer and Finnegan (2017); details are in the methodological notes of the Supplement.

The method assumed that a relatively stable ratio of sediment supply and transport capacity determined D_{50} in each reach, but transient deviations can occur (Montgomery and Buffington 1997). We thus did not expect the method to predict D_{50} at each cross section on a given day but rather as a static prediction of the long-term average. Examples of processes producing transient deviations from the average include droughts that prevent bank-full transport capacity for extended periods and wildfires that release large pulses of fine sediments from surrounding hillslopes, temporarily overwhelming the stream's transport capacity. Dams may violate the key assumption by starving the upstream supply (Kondolf 1997). Here, we assumed any such starvation was overwhelmed by sediment inputs from hillslopes and small tributaries, which seemed reasonable given the prevalence of steep slopes and wildfire in the watershed.

Water temperature.— To predict daily mean water temperature, we fitted nonlinear regressions to monitoring data for each river system (see Figures S.2, S.3). The regressions used spline curves (Wood 2006; O'Donnell et al. 2014; Rushworth 2017) to describe spatial autocorrelation in the stream network and the effects of covariates. Splines are flexible curves that can take a wide variety of shapes, allowing the data to "speak for themselves"; the only parametric constraint is a smoothness parameter that controls the "wiggliness" of the curve, selected to optimize out-of-sample prediction. We thinned the monitoring data to every fifth day to reduce temporal autocorrelation in the data set. Network structure followed the National Hydrography Dataset Plus, pre-processed as in Peterson and Ver Hoef (2014) and Ver Hoef et al. (2014).

For covariates, we followed O'Donnell et al. (2014) and used year to quantify overall trend and day of year to quantify the annual seasonal cycle. Day of year was treated as a cyclic covariate, meaning that the new year transition from day 365 to day 1 is constrained to be as smooth as the other parts of the curve. Other covariates were elevation and daily means for air temperature and long-wave solar radiation. Daily air temperature and solar radiation were gridded data (0.125° resolution) from the National Land Data Assimilation System (Mitchell et al. 2004). Individual covariates were removed if their removal improved the Akaike's information criterion, an indicator for the quality (precision, bias) of out-of-sample predictions. The models were then used to predict daily mean stream temperature for all days at all cross sections and were interpolated to 1-m^2 elements.

Our method assumed that streamflows were well mixed, which is generally true except during the dry season, when pools may thermally stratify. Although stratified pools can provide thermal refugia to salmonids (Nielsen et al. 1994), they typically have low dissolved oxygen concentrations (Smith 1990; Matthews and Berg 1997) that are probably inconsistent with use by high densities of salmon (Sergeant et al. 2017). In any case, stratification is not necessarily associated with habitat use at higher densities (e.g., Nakamoto 1994; Torgersen et al. 1999) and we therefore omitted a potential role for stratification in pools.

Incidence at capacity.— When possible, we selected the Yuba River as an ecological analog for incidence and density because (1) it is a large Sierra Nevada river used by both steelhead and spring-run Chinook Salmon; (2) Ballard et al. (2010a, 2010b) collected detailed data there on water depths and velocities used by spawners, fry, and juveniles of both species; and (3) Bratovich et al. (2012) formulated thermal criteria for salmonid performance in the Yuba River. It differs from our sites because (1) it is a tributary of the Sacramento River; (2) the local spring-run Chinook Salmon suffer from hatchery impacts (Williams et al. 2016); and (3) data for both species came from lower elevations with substantial environmental impacts (Moir and Pasternack 2008; Williams et al. 2016). Even so, it was the closest analog for spring-run Chinook Salmon because the San Joaquin River system has no extant populations, the large Feather River population has even greater hatchery impacts, and other Sacramento River populations are confined to smaller creeks (Williams et al. 2016), where annual discharges and channels are smaller and the incidence of fish in deeper habitats cannot be assessed. Steelhead are more widely distributed in the Central Valley (Williams et al. 2016) and could perhaps use a different ecological analog, but we kept the Yuba River to maintain consistent data sources and methods across the two species.

Our approach for the development of incidence functions depended on the available data. The most complete data were water depths and velocities available to and used by rearing fry and juveniles of each species, which we obtained from Ballard et al. (2010a) and analyzed with binomial regression. Their sampling design had multiple episodes during 2004–2005 and a complex structure, but we could still estimate curves with properly scaled P_{max} by adding sampling weights to our regressions and treating sampling episode as a categorical predictor. We inferred sampling weights from their methods description, following a standard scheme for use/availability data (Hosmer et al. 2013: Chapter 6). We captured sampling episodes using a categorical predictor, which allowed the regressions to retain the shape of the linear predictor from episode to episode but with different intercepts. We interpreted the largest intercept of each regression as the

incidence at capacity for that life stage and species. This is conservative because the highest observed incidence could easily be less than capacity, but by how much we cannot say precisely. During the 2004 spawning season of Chinook Salmon in the same section of river, Moir and Pasternack (2008) saw numerous superimposed redds, suggesting that spawning adults were near their capacity and thus the production of fry and juveniles was near its maximum. If this maximum exceeded the local rearing capacity, then excess fish probably emigrated and the observed incidence would be close to capacity in the general vicinity, as juvenile salmonids can migrate both upstream and downstream on the order of several kilometers to locate vacant habitat (Anderson et al. 2013).

To estimate the incidence functions for fry and juveniles, we again used regression splines—in this case, thin-plate regression splines (Wood 2006), a kind of generalized additive model that is designed to balance the conflicting goals of matching the data while making unbiased out-of-sample predictions (Wood 2006:156). For each life stage of each species, we fitted a series of thin-plate regression spline models and ranked them using evidence ratios (Burnham and Anderson 2002:78). We ranked models with water depth only, water velocity only, both as one-dimensional curves (i.e., no interaction effects), both as a 2D surface (i.e., interaction effects allowed), and a null model (episode predictor only). The top-ranked model was then used to predict incidence at capacity, with predictions limited to the range of depths and velocities in the training data ($d < \sim 2.4$ m for fry; $d < 6.0$ m for juveniles).

Unfortunately, for redds we could not infer sampling weights and P_{max} from information in Ballard et al. (2010b) because they modeled their data for available depths and velocities. They could use it to infer relative suitability, scaled arbitrarily between 0 and 1, but we could not infer the specific scaling for incidence. However, in the same channel during the same season, Moir and Pasternack (2008) saw numerous redds superimposed in the most preferred sections, leading us to reason that P_{max} is equal to 1.0 or nearly so.

For the holding stage of adult Chinook Salmon, we could not find use–availability data for depths and velocities in the Central Valley, so we derived simple threshold models from descriptive accounts (Table S.3). These accounts varied, so we examined two alternative models: a slow-pool model based on Cain et al. (2015) and Cresswell (2004) and a swift-pool model based on Moyle (2002). Besides depth, riparian trees and instream boulders are also sources of cover exploited by holding salmonids, such as steelhead (Nakamoto 1994), but adult spring-run Chinook Salmon appear to mostly use deep pools for cover. For example, 98% and 82% of holding adults, respectively, used pools for cover in the Middle and North Forks of the John Day River in 1994 (Torgersen et al. 1999). Therefore, we assumed that depth, velocity, and temperature were the only limiting factors and we set P_{max} equal to 1.0.

Temperature suitability for all life stages of all species was also modeled as a system of thresholds using the scheme of Bratovich et al. (2012), adjusted slightly for additional information from Verhille et al. (2016) and Ward et al. (2004; see Table S.4 and notes therein). The thresholds sort habitat into optimal, tolerable, and intolerable daily temperatures. Here, "tolerable" does not imply poor habitat but simply conditions under which fish face greater stress or metabolic costs than in optimal temperatures. Thus, for optimal and tolerable temperatures we assumed that incidence at capacity arose from depth and velocity as described for the binomial regression above, but we summed the two categories separately. For intolerable temperatures, we assumed zero incidence at all depths and velocities.

Density at capacity.— For holding density, we used 1.0 fish/m^2, the midpoint of a range reported by Stillwater Sciences (2012) from aerial photos of spring-run Chinook Salmon holding in pools within Butte Creek, California. The range reported for the photos was 0.5–1.5 fish/m^2, giving some sense of uncertainty, although the SE is presumably smaller than the range. For spawning, we used the "largest movable grain" concept of Riebe et al. (2014), in which a streambed's capacity for redds arises from scaling relationships among three factors: (1) the fraction of movable grains on the streambed, estimated from D_{50}; (2) the area of a typical redd; and (3) the mean body length of spawners (for details, see methodological notes in the Supplement). Generally, mean body length of spawners depends on age composition, but age-3 and age-4 spawners tend to dominate runs of both species in the Central Valley, so we bracketed the potential mix with high and low estimates from pure age-3 and age-4 runs, respectively (for length at age, see Table S.5). For fry and juveniles, we inferred density at capacity from the Yuba River data as the mean fish density in occupied sample units (Table S.6). These means fell well within the 95% confidence bounds of an allometric equation for generic densities at capacity of rearing salmonids (Grant and Kramer 1990).

Daily and seasonal capacity.— Having estimated all parts of equation (1), we calculated daily capacities and then summarized their seasonal dynamics. In our approach, daily capacity could fluctuate dramatically from day to day and from week to week, which gave interesting insights but also raised a question: when capacity dips suddenly, can fish wait it out somehow and then use the habitat when conditions improve a few days or weeks later? This seemed a knotty question, but we had to wrestle with it to estimate seasonal capacity from the daily capacities. Rather than try to answer it definitively, we

TABLE 2. Spectrally based depth retrieval, with training and testing statistics.

Parameter	Description	Merced River	Tuolumne River
λ_1	Wavelength (nm) of optimal band in equation (2)[a]	504	490
λ_2	Wavelength (nm) of optimal band in equation (2)[a]	632.5	632.5
R^2 (train)	Variance explained by regression	0.82	0.90
σ_r (train)	Regression SE (m)	0.48	0.34
R^2 (test)	Variance of test data explained by regression	0.71	0.91
σ_r (test)	SE for test data (m)	0.48	0.33
Intercept	Linear regression of predicted versus measured	0.30	−0.0093
Slope	Linear regression of predicted versus measured	0.82	1.01

[a]See also Figure S.4 and Richardson (2016) for additional details on optimal band ratio analysis and validation procedures.

assessed its importance by generating low, medium, and high estimates of seasonal capacity. Low seasonal capacity was the daily capacity at which only 5% of daily capacities were smaller over the typical season for a particular life stage in a particular year (i.e., it is the 5th percentile). It treats the life stage as highly sensitive to dips. The high seasonal capacity was the median daily value (the 50th percentile) and thus treats the life stage as indifferent to dips and spikes (the latter helps as much as the former hurts). Finally, the medium seasonal capacity was between these two (the 25th percentile).

We also asked whether capacities were sensitive to systematic error in the modeled flow fields. Daily capacities were re-estimated from flow fields in which all depths or all velocities had been adjusted by −10, −5, +5, or +10%. Over this range, the proportional change in the capacities was approximately linear; therefore, a sensitivity index s was defined as the slope of a linear regression for proportional response ($\%\Delta Y$ per $\%\Delta X$).

RESULTS

Physical Traits of the Reintroduction Areas

Channel bathymetry.— The optimal colors (λ_1 and λ_2) for retrieving water depths from images were similar in the two river systems (Table 2), but they predicted d slightly better in the Tuolumne River (R^2 in Table 2). The Merced River regression tended to overpredict shallow depths less than 0.3 m and to underpredict depths greater than 2.5 m, perhaps due to radiance saturating in deep water. The Tuolumne River regression gave highly accurate depths (Table 2). You can observe the detail of the depth maps in Figure 2, where pools of various sizes and shapes alternate with shallow riffles and runs. Entire DEMs can be downloaded from the U.S. Geological Survey's ScienceBase Catalog (Legleiter et al. 2020).

Water depths and velocities.— To show overall patterns (Wyrick et al. 2014), we condensed the modeled flow fields into rating curves for four broad types of hydraulic habitat (Figure 3). Deep–slow and shallow–slow habitats persisted in both rivers up to discharges of about 10 m^3/s (Figure 3A, C), although they shrank rapidly above 3 m^3/s. Shallow–swift habitat swelled over this same range from a few hectares per river to about 50 ha. Deep–swift habitat rapidly dominated in both rivers at discharges greater than approximately 30 m^3/s, and the slow habitats nearly disappeared. However, a small portion of shallow–slow habitat persisted in overbank areas even at the highest discharges (Figure 3B, D).

Grain size.— In the predictions for D_{50}, all five channels showed a general pattern of upstream coarsening, although with much local variation (Figure 4). Grain size tended to be coarser and less spatially variable in the Tuolumne River system, with the D_{50} of the median cross section being 73% higher than that in the Merced River (D_{50} = 64 mm versus 37 mm; see Table 3). Even so, the fraction of movable grains for spawners was generally high enough to provide widespread spawning substrates in both systems—at least 56% of the channel for steelhead and 67% of the channel for Chinook Salmon (Table 3).

Water temperature.— Adjusted R^2 values in the temperature regressions were high: 0.81 for the Tuolumne River and 0.94 for the Merced River (see Table S.7 for regression summary). In each, removing any covariate worsened the Akaike's information criterion, showing that all five covariates added value to out-of-sample predictions. The spline curves for air temperature and long-wave radiation (not shown) were nearly linear and similar across the two systems, and within the reintroduction areas the curves for elevation showed the expected inverse trend with temperature.

The temporal covariates were interesting. For the year covariate, the Tuolumne River had a smoother curve (Table S.7; smoothing parameter = −6.89 versus the Merced River's −16.11), suggesting that it resisted year-to-year variability in unmodeled drivers, such as annual discharge or snowpack. The day-of-year covariate revealed an annual temperature cycle that spanned only 12°C in the Tuolumne River versus 19°C in the Merced River (Figure 5), and the Tuolumne River's annual mean was cooler as well, by 1.6°C (Table S.7, model terms).

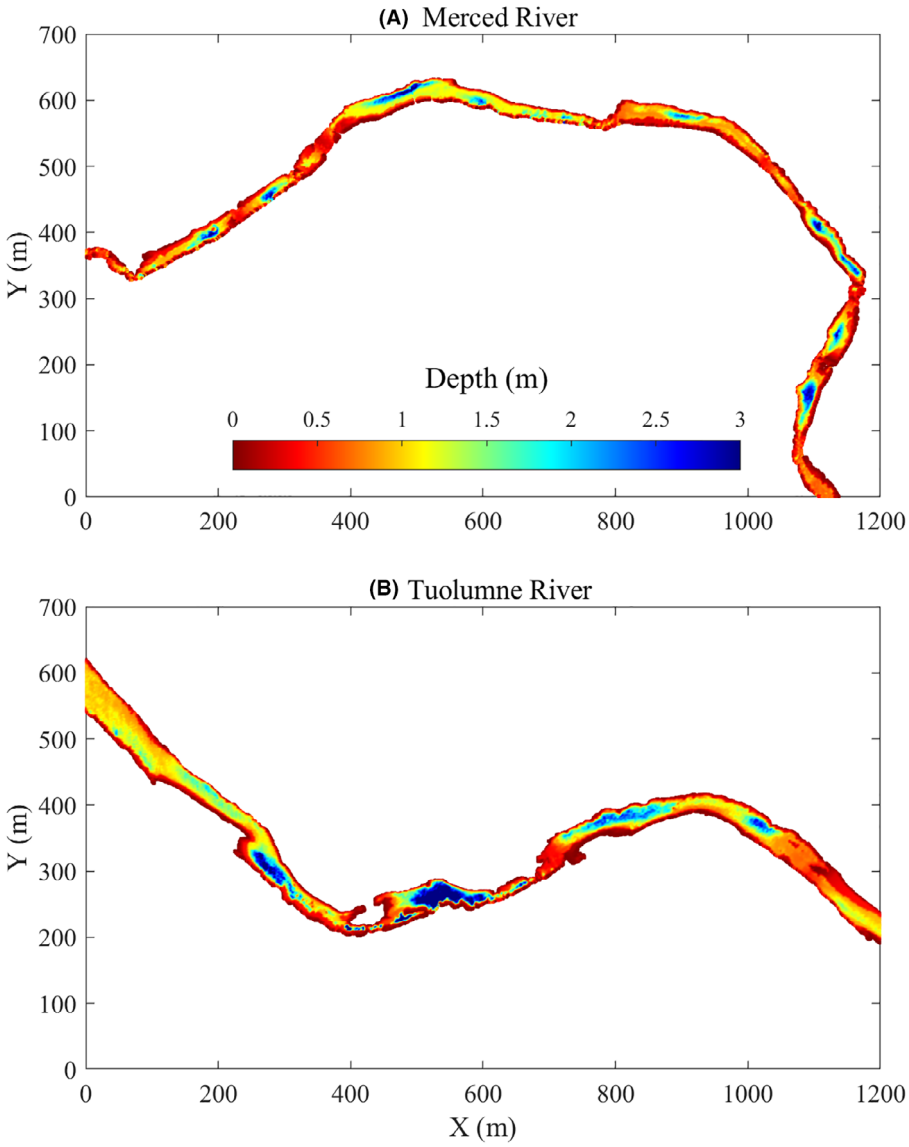

FIGURE 2. Representative segments of the water depth maps computed from hyperspectral images of the **(A)** Merced River and **(B)** Tuolumne River. Flow is right to left, and depths describe bathymetry at the time of remote sensing (September 2014).

However, within each day of year, the Tuolumne River's predicted temperatures had an SD about 2.5 times wider than that of the Merced River (shading in Figure 5), mostly from spatial variation. We inspected the monitoring data for clues and concluded that two outfalls from hydroelectric tunnels in the Tuolumne River produced these differences from the Merced River.

Incidence Functions for Fry and Juveniles

For incidence, we report only the new regressions for fry and juveniles. For Chinook Salmon, the top-ranked models (evidence ratio = 1) had the same structure for fry and juveniles (Table 4). In both models, incidence depended on both depth (d) and velocity (v), but their effects were additive (no interaction), and the v-spline looked just like a linear response (i.e., logistic curve had an evidence ratio = 1). The prediction surfaces for fry and juveniles had broadly similar shapes (Figure 6, middle), but juveniles tolerated deeper, swifter water. For steelhead fry, the top-ranked model also had the same structure (Table 4), but steelhead juveniles shifted to a distinctly different incidence, with a 2D surface (interaction effect) greatly outperforming the other models (Table 4, rightmost column). The prediction surface (Figure 6, bottom)

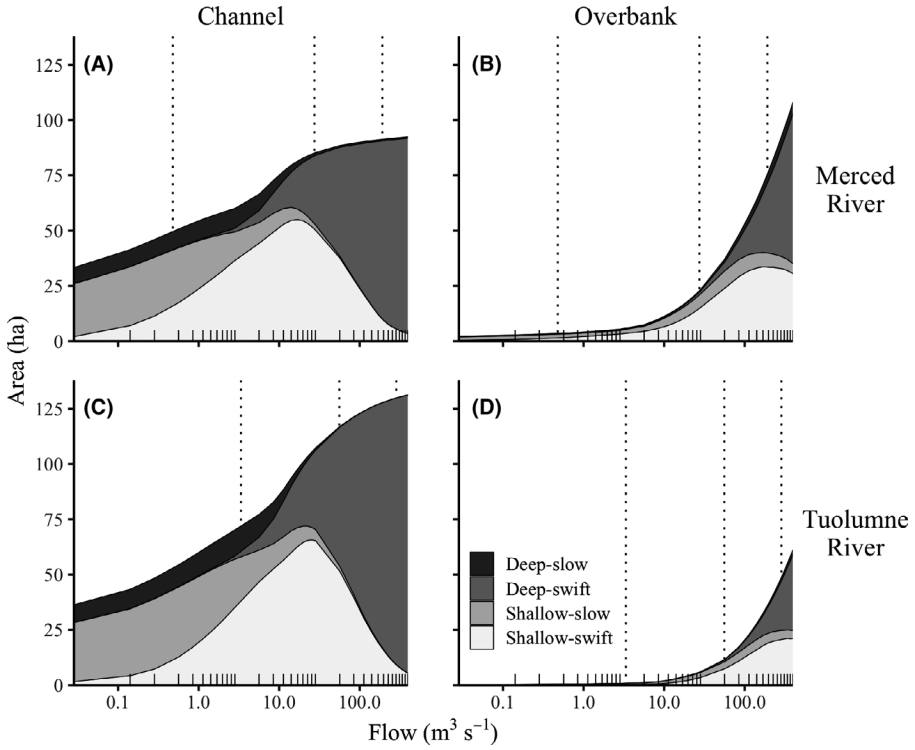

FIGURE 3. Rating curves for four hydraulic habitats, defined by deep versus shallow (cut-off: depth $d = 1.0$ m) and slow versus swift (cut-off: velocity $v = 0.25$ m/s), in the main stem of each river (Merced and Tuolumne rivers). Vertical dotted lines show the averages of yearly minimum, mean, and maximum daily discharges over 2008–2017. Due to flow regulation, the Tuolumne River tends to maintain a substantially higher minimum and mean discharge relative to the natural hydrograph of the Merced River. The rug plot along the *x*-axis in each panel marks the design flows from which the plots were interpolated.

revealed that juveniles shifted their hydraulic niche to specialize on shallow, high-velocity areas. This showed clearly that the hydraulic niches of steelhead and Chinook Salmon began similarly but then diverged.

The regressions inferred P_{max} values ranging from 0.55 in Chinook Salmon juveniles to about 0.78 in Chinook Salmon fry (Figure 6, bottom), with steelhead being intermediate, each inferred from the sampling episode with the largest intercept. The pattern of intercepts (fixed effects) in the Yuba River data generally agreed with life history timing (Figure 6, top). The greatest incidence of Chinook Salmon fry was in March 2004, immediately after the peak incubation season; the incidence of juveniles peaked 2 months later in May 2004. However, the highest peak for juveniles came in September 2005—presumably yearling fish that were concentrated to high incidence by dry season flows. For steelhead, the highest incidences were July 2004 for fry and November 2004 for juveniles (Figure 6, top), consistent with the timing of life history and streamflow. The fact that the peak incidence of juveniles in both species arose during the seasonal bottleneck of low flow (September, November) reassured us that incidence at capacity was a reasonable interpretation.

Capacities for Spring-Run Chinook Salmon

Holding.— Patterns of adult holding capacity varied across years and model assumptions but reliably favored the Tuolumne River. In both the extreme drought and wet years, the Merced River system became thermally intolerable at the height of summer (Figure 7, left column), while the Tuolumne River always maintained at least some tolerable and optimal holding capacity (Figure 7, right column). In fact, in all 10 years the summer holding capacity of the Merced River always went to zero for extended periods (Table S.8, top). The Tuolumne River generally maintained capacity in the thousands or tens of thousands of fish, although capacity under the slow-pool model occasionally dipped to 700 or 800 fish in wet years (2011 and 2017; Table S.8, bottom). These dips stemmed from water releases that were large enough to convert pools from slow to swift.

Spawning.— Patterns of spawning capacity generally favored the Tuolumne River. Here, we focus on patterns for age-3 spawners; patterns for age 4 were similar but smaller by 27% due to larger redd size. During the peak season from mid-September through October, the low seasonal estimate (5th percentile of daily capacity) dropped to

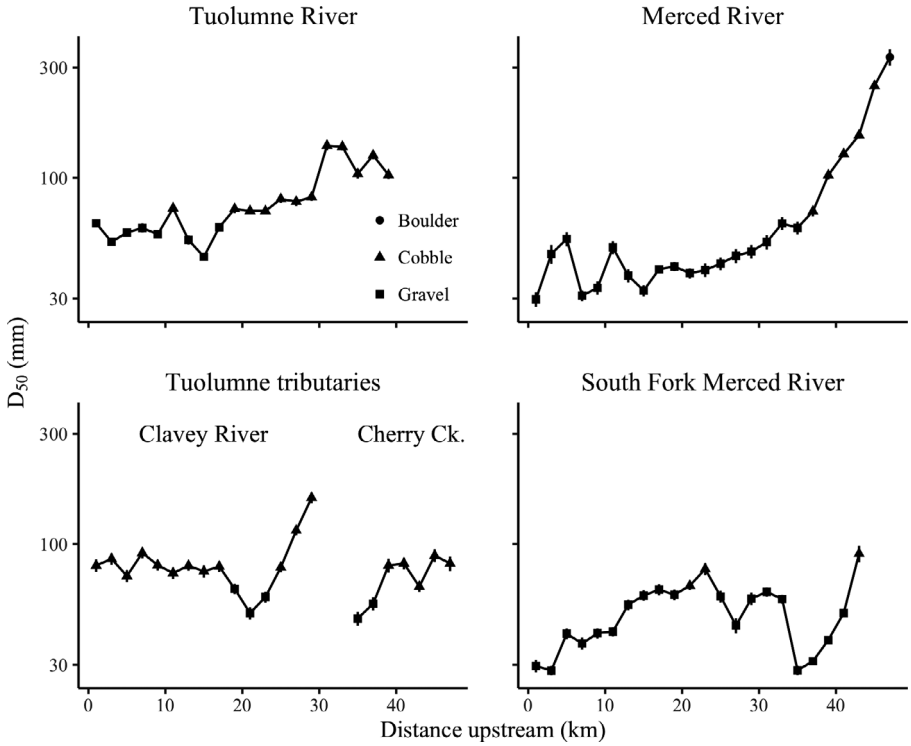

FIGURE 4. Predictions of median grain size (D_{50}) aggregated for each 2-km section of channel. Standard errors are due to variation in D_{50} among individual cross sections, numbering approximately 67 cross sections/km. The upstream end of each series marks the approximate second-order limit to migration, except for the South Fork Merced River, where Peachtree Falls limits migration at river kilometer 14.6. Cut-off points (D_{50}) are 256 mm between boulders and cobble and 64 mm between cobble and gravel.

zero redds in the Merced River during half of the years but always stayed above 3,000 in the Tuolumne River (Table S.9). The high seasonal estimate (50th percentile) was 4–680 times larger in the Tuolumne River depending on the year. Comparing the Merced River in extreme drought and wet years, the drought year saw no suitable temperatures for spawning until mid-October (Figure 8A), a full month from the model's assumed start of the peak spawning season and just 2 weeks before its end. The wet year (Figure 8C) saw pulses and dips in capacity during early October, which would allow thousands of fish to spawn in weeklong windows, but September was still too warm. In contrast, the Tuolumne River kept thermally optimal capacity for at least 5,000 redds throughout the spawning season in both years (Figure 8B, D). In both river systems, temperature and flow patterns greatly expanded capacity in November, after the end of the spawning season, suggesting that if spring-run Chinook Salmon could delay their spawning, they would benefit from many more options.

Fry.— During the extended fry season from November through March, daily mean water temperature was always tolerable or optimal in both systems during all years. The Merced and Tuolumne rivers had similar capacities. Daily capacity usually fell between 2 and 3 million fry except after storms, when high velocities drove capacity down in reverse spikes (Figure 9). In most years, these spikes were short-lived, but during the wet years of 2011 and especially 2017, the capacity dropped for weeks at a time (Figure 9).

Juveniles.— For subyearlings, spring capacity ran about an order of magnitude smaller than fry capacity (Table S.10, top). Over 10 years, the high seasonal estimate (50th percentile) never fell below 175,000 fish in either system and averaged 300,000 in the Merced River and 350,000 in the Tuolumne River. These spring capacities were also relatively stable: the medium estimate averaged 86% of the high estimate in both systems, and the low estimate averaged at least 62% of the high estimate. In contrast, the summer capacities for yearlings (Table S.10, middle) were smaller and less stable, especially in the Merced River, where they peaked in the hundreds and often fell to zero due to temperature (see Figure S.6, panels A, C versus panels B, D). The Tuolumne River maintained a higher, more stable capacity over the summer and into the fall (Table S.10, middle and bottom).

Capacities for Steelhead

Spawning.— Compared to Chinook Salmon, steelhead in their peak season had ample spawning capacities spread over a cooler time of year. Even in their worst year, the

TABLE 3. Predicted median grain size (diameter D_{50}) and fraction of movable grains (F_m) for each river system.

Predicted quantity	Merced River system[a]	Tuolumne River system[b]
Bank-full area (ha)	122	198
D_{50} (mm)[c]		
5th percentile	13	26
50th percentile	37	64
95th percentile	182	178
F_m (SE)[d]		
Chinook Salmon (age 3)	0.76 (0.003)	0.67 (0.002)
Chinook Salmon (age 4)	0.77 (0.003)	0.70 (0.002)
Steelhead (age 3)	0.67 (0.003)	0.56 (0.002)
Steelhead (age 4)	0.70 (0.003)	0.60 (0.002)

[a]Omits an inaccessible channel above Peachtree Falls.
[b]Includes the Clavey River channel.
[c]Percentiles for distribution among cross sections (weighted by bank-full area for each cross-section); $n = 4{,}056$ (Merced River) and 5,415 (Tuolumne River) cross sections.
[d]Mean and SE weighted by bank-full area for each cross section. The F_m of cross sections was estimated as described in the Supplement equation (4), and grain size D_{84} was obtained as in Figure S.5.

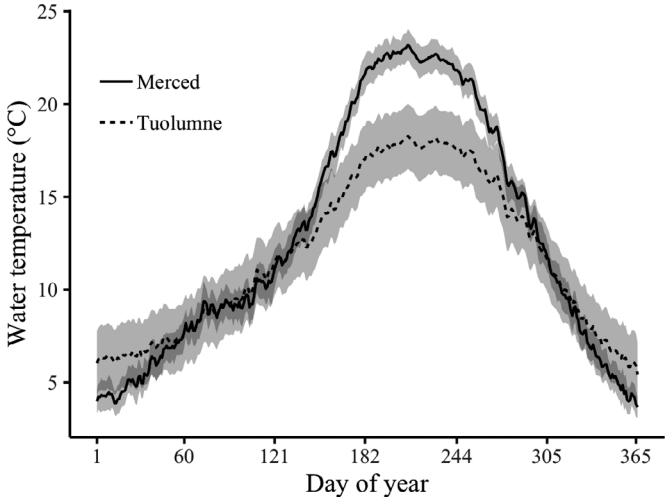

FIGURE 5. Mean daily stream temperature predicted from the network regressions for the main stem of each river (Merced and Tuolumne rivers) downstream of secondary migration barriers. Lines show the mean daily temperature across all cross sections and years for a given day of year; shading shows 0.5 SD on either side of the mean.

high seasonal capacity for age-4 steelhead was 45,000 redds in the Merced River and 70,000 redds in the Tuolumne River (Table S.11); the mean of the high estimate across all years was double these amounts. The low and medium seasonal estimates were also robust, always staying in the tens of thousands in both drainages. In the early and late seasons, however, the Merced River's low and medium estimates shrank drastically (Table S.11),

TABLE 4. Evidence ratios for regression models of rearing habitat. Models are ordered from least complex to most complex; evidence ratios are relative to the best model of the set.

	Evidence ratio against[b]			
	Chinook Salmon		Steelhead	
Candidate models[a]	Fry	Juveniles	Fry	Juveniles
Null model	8×10^7	6×10^4	10^8	6×10^3
d curve only	9×10^4	7.2	15	13
v curve only	950	4×10^4	4×10^7	1.5×10^4
d curve, v linear[c]	1.0	1.0	1.0	27
Two one-dimensional curves	1.0	1.0	1.0	27
Two-dimensional surface	1.8	13.6	6.6	1.0

[a]d = water depth as predictor; v = water velocity as predictor.
[b]Evidence ratio of 1.0 indicates the top-ranked model(s) for that model set.
[c]Added post hoc to check for equivalence with two one-dimensional curves.

suggesting that the Tuolumne River would support a greater diversity of spawn timing. For the early season, this difference stemmed from both hydraulic and thermal conditions, but for the late season it was simply thermal (Figure S.7).

Fry.— Daily fry capacity tended to fall between 1.0 and 1.5 million in both systems, except for contractions during storms in the wet season and snowmelt or intolerable temperatures in the dry season (Figure 10). The drought years (2012–2016) tended to drive fry capacity down during the late summer in the Merced River but not in the Tuolumne River, where capacity stayed above 1.0 million. In wet years (2011 and 2017), fry capacity dropped for long periods in both systems due to swift water.

Juveniles.— Overall, juvenile capacity ran about an order of magnitude smaller than fry capacity (Table S.12). The high seasonal estimate (50th percentile) averaged across the 10 years was smallest during the summer quarter in the Merced River (204,000) but smallest during the spring quarter in the Tuolumne River (341,000; the summer quarter was similar at 348,000). Generally, the Tuolumne River tended to hold a larger, more stable capacity (see Table S.12, "mean relative to high"), particularly in spring and summer.

Sensitivity to the Modeled Flow Field

The sensitivity index s (Figure 11) showed the response of capacity estimates to systematic errors in depth or velocity: an s of 0 implies no sensitivity; an $|s|$ equal to 1 represents symmetric sensitivity (e.g., 5% error in predictor translates to 5% error in capacity); and an $|s|$ less than 1 or greater than 1 represents weak or strong sensitivity. The sign of s indicates the direction of the response.

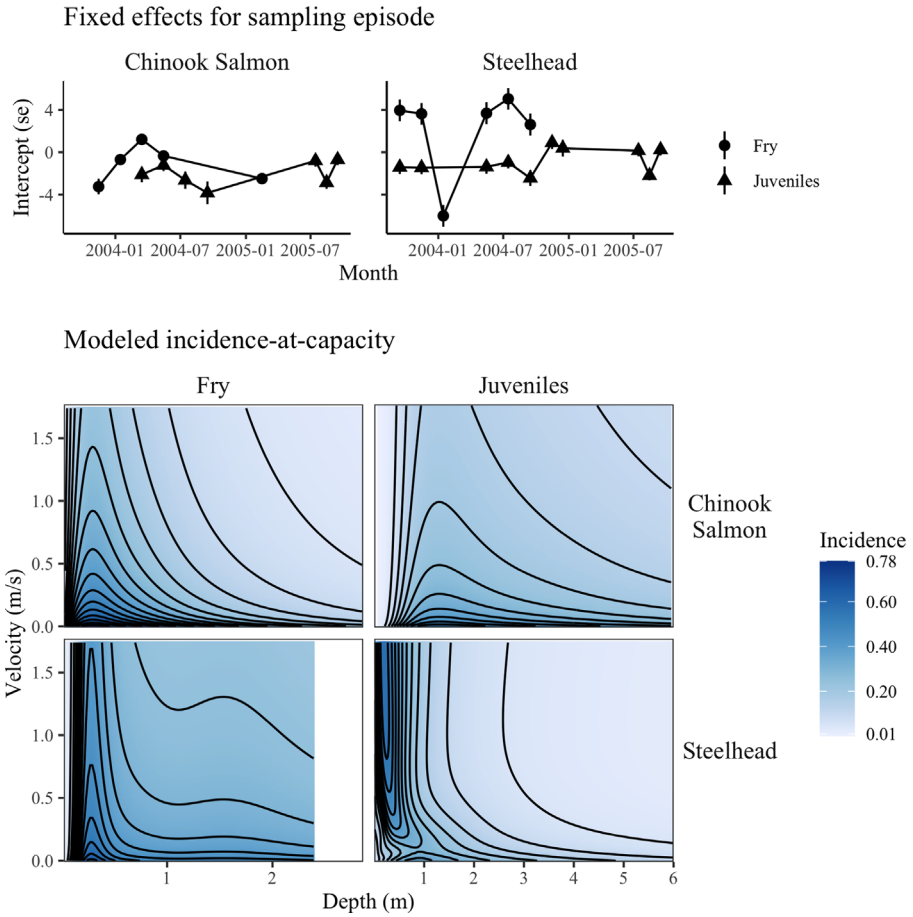

FIGURE 6. Incidence models for fry and juvenile Chinook Salmon and steelhead as a function of water depth and velocity. Top panels depict the fixed effects of sampling episode, estimated in the binomial model and interpreted as relative incidence at different times of year. Bottom panels show the estimated response surface for the sampling episodes with highest incidence, interpreted as incidence at capacity. Contours are separated by 0.05 probability units; the darkest shading represents P_{max}. Predictions are masked to the range of depths and velocities in the training data.

For Chinook Salmon, the sensitivity of holding and spawning capacity was weak to nonexistent except for holding capacity in the Tuolumne River, which could be strongly sensitive to error in both predictors (Figure 11, top right). For fry, sensitivity was weak, although for velocity it was nearly symmetric; for juveniles, it was usually close to symmetric (Figure 11, middle rows).

For steelhead spawning, fry, and juveniles, sensitivity ranged from nonexistent to nearly symmetric (Figure 11, bottom rows). The largest *s*-values were for spawning capacity and depth errors, fry capacity and velocity errors, and the low estimates of juvenile capacity and velocity errors.

DISCUSSION

Capacity for steelhead in both systems appeared to be well above the criteria for viability, estimated by Lindley et al. (2007) to be 2,500 spawners/generation or 600–800 spawners/year. We inferred capacity for redds in the tens of thousands, fry in the low millions, and juveniles in the hundreds of thousands in both river systems, suggesting the potential for creation of a productive resource. Populations of *O. mykiss* already inhabit both of these systems, pursuing a non-anadromous, freshwater-resident life history (i.e., Rainbow Trout) but retaining the genetic basis for anadromy (Pearse and Campbell 2018). *Oncorhynchus mykiss* with anadromous alleles apparently migrate downstream to reside in reservoirs (Leitwein et al. 2017; Pearse and Campbell 2018) such that re-establishment of anadromous steelhead could potentially emerge simply from diverting these downstream migrants to the lower river via a fish collector at the head of the reservoir and providing means for upstream passage to the adult steelhead that eventually return (Kock et al. 2021). A fish collector at the forebay next to the dam would probably be less effective

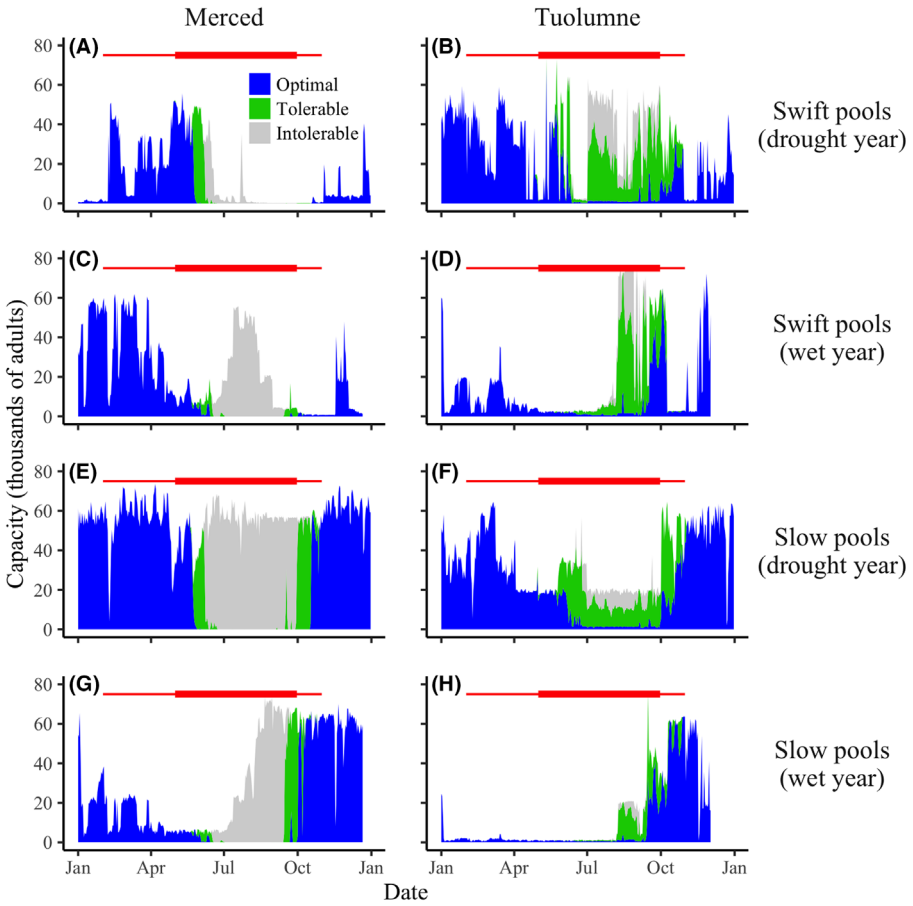

FIGURE 7. Daily holding capacity for adult Chinook Salmon during the peak (thick red line) and extended (thin red line) holding season. Panels compare the Merced and Tuolumne River systems in a wet year and a drought year and contrast predictions from two alternative habitat models. Colors show how much of the hydraulic capacity met the thermal criteria, with gray areas indicating suitable water depths and velocities but intolerable thermal conditions.

due both to the propensity of migrants to stop in the reservoir and the large size of the forebay, which reduces the effectiveness of fish collectors (Kock et al. 2019).

Capacity for Chinook Salmon in both systems was ample for fry and subyearlings, numbering in the millions and hundreds of thousands, respectively. In contrast, for adults the two rivers diverged. The Merced River was too warm for holding and nearly so for spawning, while the Tuolumne River usually maintained holding and spawning capacity in the thousands or tens of thousands per year, well above the criteria for viability. However, these important findings depended on the limited information underlying our threshold models for the adult stages, which we discuss further below. The thermal conditions were also considerably more favorable in the Tuolumne River for yearling juveniles, especially during dry years, when this form is especially important for sustaining adult production (Cordoleani et al. 2021). Overall, this suggests that the Tuolumne River could support a more stable and resilient population of spring-run Chinook Salmon than the Merced River.

The high-resolution approach gave some interesting insights into physical constraints on each species' expression of life history. Adult steelhead exploit a long window during the wet season to migrate and spawn (McEwan 2001), with the result that their fry are exposed to the high water velocities of snowmelt and the warm temperatures of late summer (Figure 10). However, by the beginning of the next wet season, the juvenile fish have specialized on swift water (Figure 6); this, combined with their thermal tolerance, opens up a strategy of staying one or more full years in the rivers (Lee 2020). Spring-run Chinook Salmon, in contrast, spawn within a short window at the start of the wet season (Garman and McReynolds 2009). This allows their progeny to squeeze their freshwater rearing into a single wet season while avoiding warm summer temperatures, at least for the subyearling form (Moyle 2002). The strategy also exposes the holding and spawning

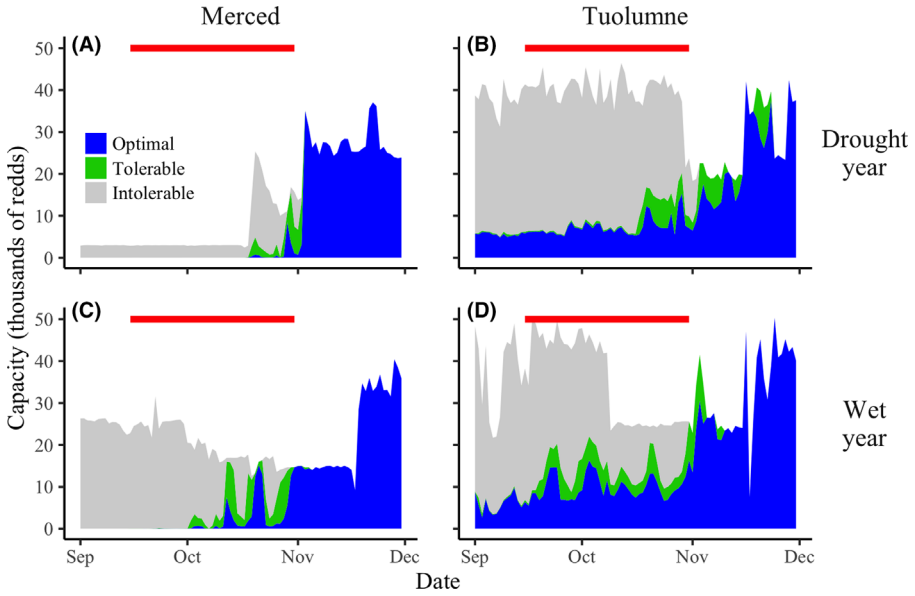

FIGURE 8. Spawning capacity modeled for age-3 spring-run Chinook Salmon during **(A)**, **(B)** the drought year 2015 in the Merced and Tuolumne rivers and **(C)**, **(D)** the wet year 2017 in each river. Red bars show the extent of the spawning season. Colors show how much of the hydraulic capacity met the thermal criteria, with gray areas indicating suitable depths, velocities, and spawning substrate but intolerable temperatures.

stages to warm temperatures (Figures 7, 8) and exposes the fry to spikes in water velocity during winter storms (Figure 9).

Physical Predictors

Our results ultimately depend on accurate bathymetry. Hyperspectral imagery has already produced accurate depth maps for gravel-bedded rivers (Legleiter et al. 2009; Legleiter and Harrison 2019), but here we have shown similar accuracy to be feasible in steep mountain rivers with coarse beds. As in prior work (Legleiter et al. 2018; Legleiter and Fosness 2019), our maximum predictable depth was about 2.5–3.0 m, meaning that pools that were actually deeper were likely assigned depths in the range of 2.5–3.0 m. Thus, their modeled depths would be too shallow and would predict water velocities too swift due to the nature of the hydraulic model. This bias for depth was in low-incidence regions of the spawning and rearing models (much deeper than typically used), so the estimates of capacity would likely be insensitive to it. For the holding models, the bias would occur at depths 0.5–1.0 m below the threshold for suitable habitat (1.5–2.0 m deep, depending on the model), and so these deepest pools would still classify as suitable habitat. The bias for velocity, however, may have depressed the estimates from the slow-pool model in the Tuolumne River, which were quite sensitive to systematic error in velocity (Figure 11, top right panel). The slow-pool estimates in the Merced River were weakly sensitive, probably because pools were usually too warm irrespective of hydraulics.

In fact, the Merced River's warmer flows during the dry season, as summarized in Figure 5, drove many of the differences in capacity between the two systems. Why was the Merced River so much warmer than the Tuolumne River in summer and slightly cooler in winter? The underlying mechanism for thermal buffering of the Tuolumne River appeared to be the system of tunnels feeding water from three high-altitude reservoirs to hydroelectric powerhouses near the confluence of Cherry Creek and Tuolumne River, part of the Hetch Hetchy System that supplies water to San Francisco (Hanson et al. 2005; Righter 2005). Because subsurface rock is generally cooler than the surface in summer and warmer in winter, surface water flowing through the tunnels would tend to lose heat to the surrounding rock in summer and absorb it in winter, passively buffering its temperature (Figure 12). This sort of back-and-forth passive heat exchange occurs between normal rivers and their beds, slightly moderating both diurnal and seasonal temperature swings (Pike et al. 2013). The tunnels buffer more strongly by penetrating deeper, more thermally stable layers of rock as well as blocking direct energy inputs from the atmosphere, producing an average temperature drop of 5°C at the height of summer (Figure 12), when it would matter most for yearling juveniles and holding adults. The current operations of the Hetch Hetchy System thus appear to produce a thermal effect similar to groundwater, which can be beneficial to the persistence of salmonid populations (Torgersen et al. 1999; Ebersole et al. 2003).

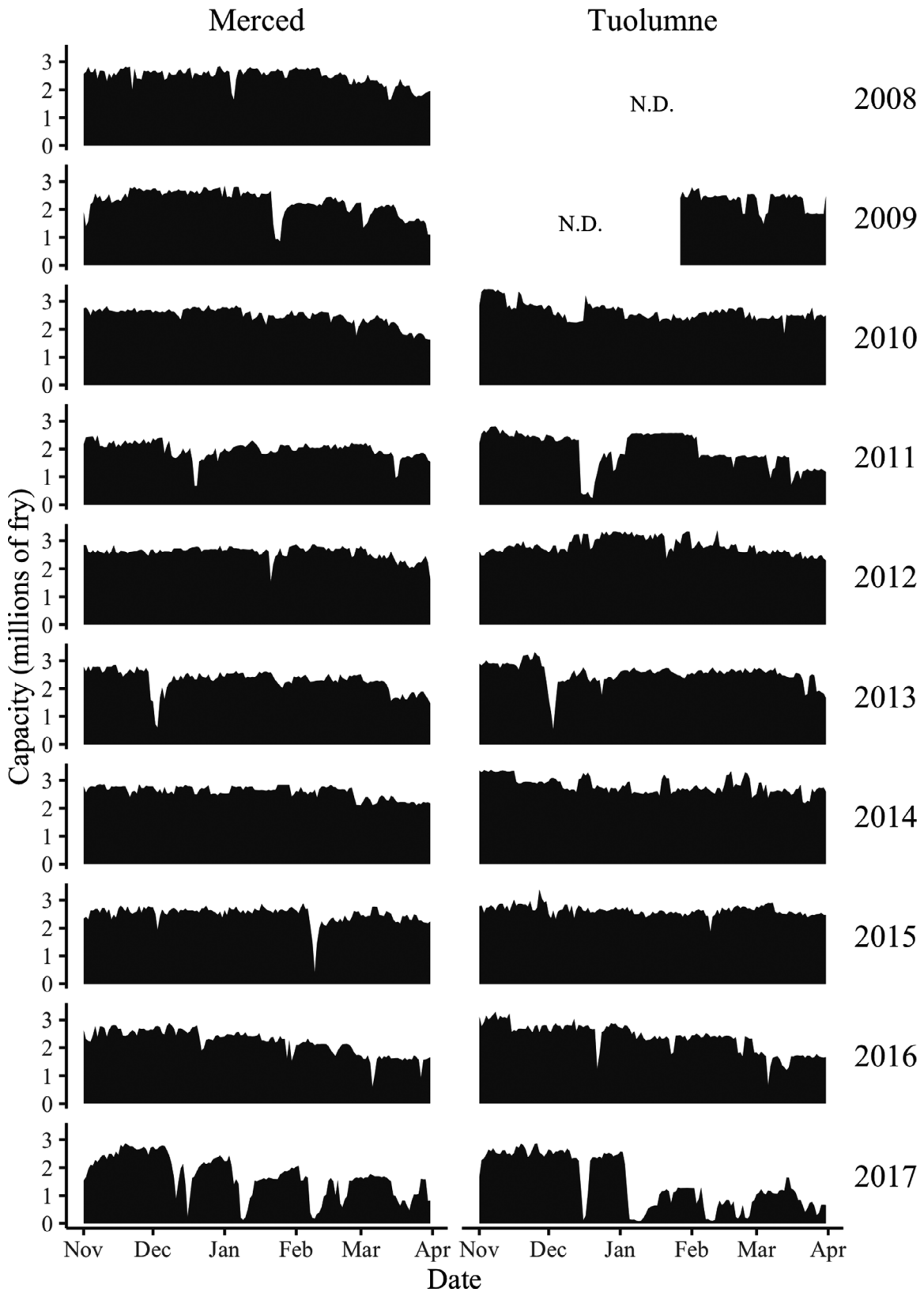

FIGURE 9. Daily fry capacities in the Merced and Tuolumne rivers modeled for spring-run Chinook Salmon during their full rearing season for each of 10 years (N.D. = no data). Peak season is December–February.

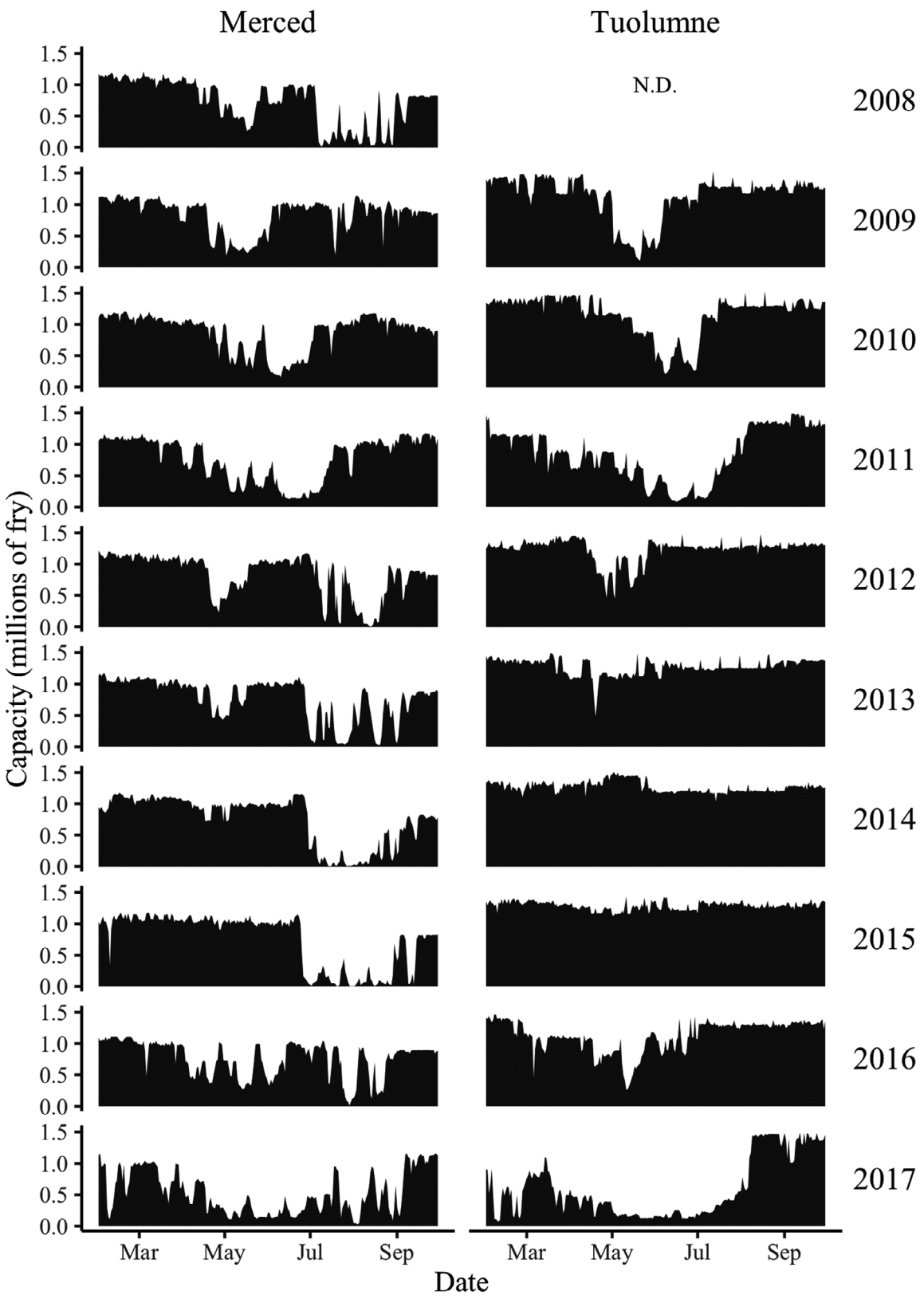

FIGURE 10. Daily fry capacities in the Merced and Tuolumne rivers modeled for steelhead during their full rearing season for each of 10 years (N.D. = no data).

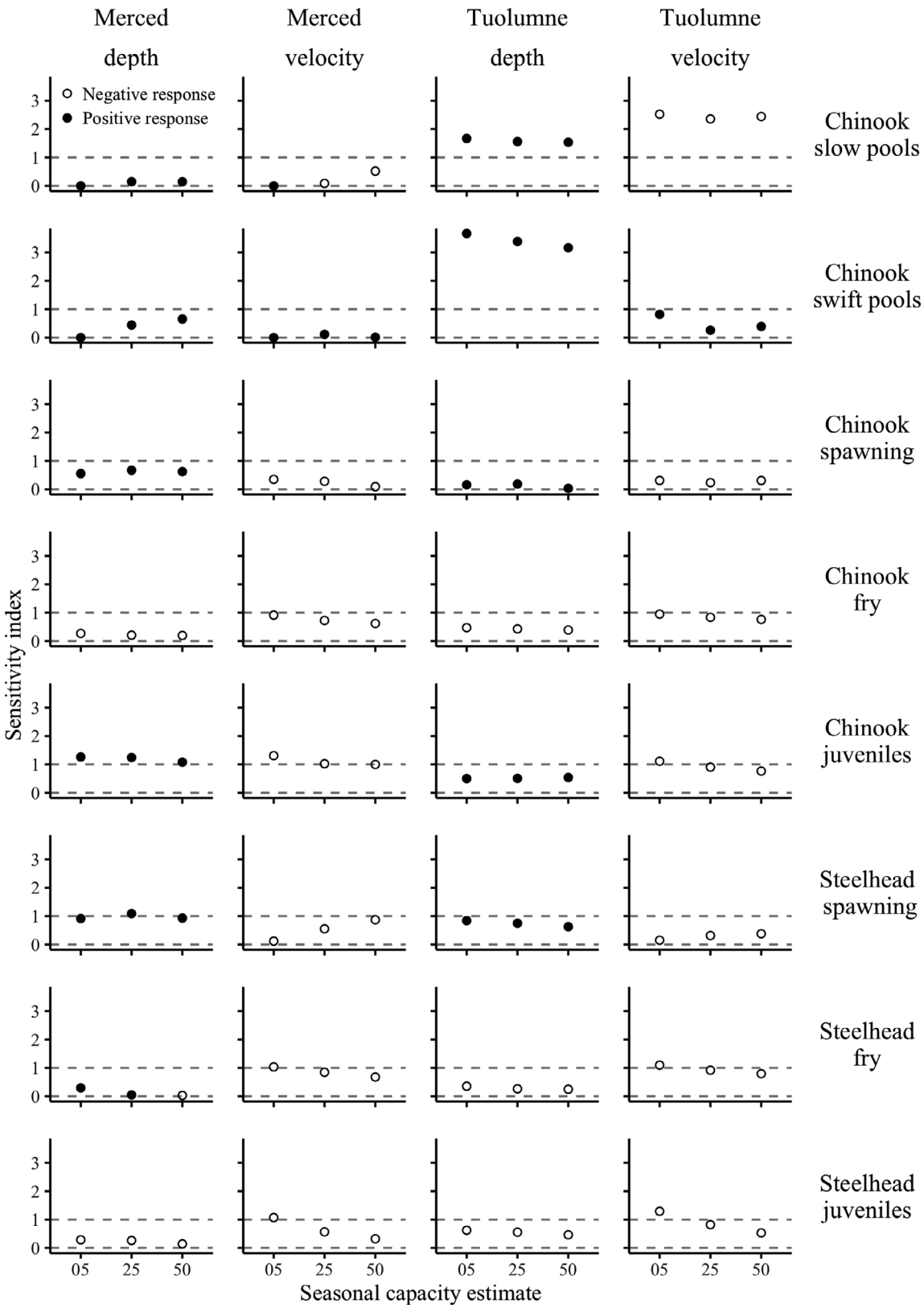

FIGURE 11. Sensitivity of the capacity estimates to systematic error in modeled depths or velocities. Dashed lines identify insensitivity ($|s| = 0$) and symmetric sensitivity ($|s| = 1$).

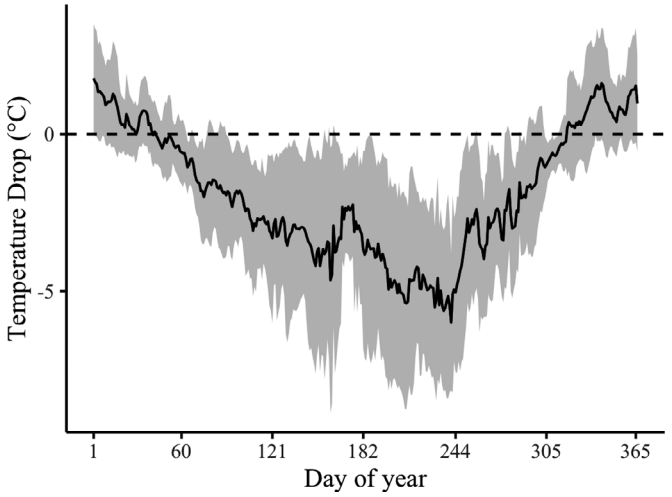

FIGURE 12. Passive thermal buffering of streamflows near the confluence of Cherry Creek and the Tuolumne River, stemming from current operations of the Hetch Hetchy System at Early Intake (Holm and Kirkwood powerhouses, Early Intake water diversion to the Mountain Tunnel; Hanson et al. 2005). Shown is the daily mean temperature drop for the combined flow of Cherry Creek and the Tuolumne River at Early Intake, estimated from stream gauges immediately above (U.S. Geological Survey [USGS] 11278300 and 11276600) and below (USGS 11278400 and 11276900) the facilities. Daily means are for the years 2011–2020 (the approximate period of record); shading shows the SD among years.

Wild Chinook Salmon and the Wild Merced River

In contrast to the Tuolumne River, the upper Merced River's temperatures represent a natural pattern, since its flow and thermal regime is one of the least impaired of any large river system in the Sierra Nevada. Why is it too warm for Chinook Salmon to hold and spawn? Given that spring-run Chinook Salmon used the upper Merced River in the 19th century and likely outnumbered the fall run (Yoshiyama et al. 2001), we see two possibilities: either the system has warmed or our assumptions about adult Chinook Salmon were wrong.

Changing climate potentially could have warmed the upper Merced River. We lack the data on river temperature to check this directly, but we can check it indirectly by looking at a century of discharge records and air temperatures (Figure 13). Climate warming should diminish snowpack relative to total rainfall, shrinking the proportion of annual discharge occurring after April 1—the conventional date that marks the peak snowpack in the Sierra Nevada. We do see this signature at the Pohono Bridge gauge in Yosemite Valley (Figure 13A), although during 2008–2017 about half the years still fell within the range from a century ago. However, accelerated snowmelt did not appear to alter the low discharges later in the dry season, since we saw no overall trend in the lowest monthly discharge from June to October (Figure 13B). The decadal means for air temperature in July and August have trended upwards in recent decades in Yosemite Valley and the City of Merced on the Central Valley floor (black lines in Figure 13C, D), but individual years still fall within the range of historic variability (gray dots in Figure 13C, D). The trend is driven by cool years becoming rare, not by warm years becoming warmer. We conclude that climate warming, though present, cannot completely explain why temperatures in the Merced River were uniformly intolerable for holding Chinook Salmon over 2008–2017 (Table S.8)—although the loss of cool years may partially explain it.

The river system may have lost riparian trees and shading due to human activity, but we find little evidence for this. Despite a highway and an abandoned railway on either side of the Merced River, our imagery revealed riparian tree cover to be similar to the remote channels of the South Fork Merced River and the main-stem Tuolumne River, where it was very low due to sparse trees and a wide channel. Placer mining in the 19th century likely affected riparian tree cover in both rivers, but the mining districts were downstream of our spatial extent (Lang 1882; Koschmann and Bergendahl 1968). We suggest that shading may be naturally low but is poorly studied in these larger Sierra Nevada rivers.

More likely, the thermal tolerances we assumed for holding and spawning were too restrictive, either because extant populations of spring-run Chinook Salmon are poorly characterized or because they differ from the extinct populations of the San Joaquin River system. For holding, we inferred tolerance limits from a population in Butte Creek, a northerly tributary of the Sacramento River, where Ward et al. (2004) reported 3 years with similar run sizes but different mortality of holding adults (Table 5). Deaths of holding adults tended to appear in the weeks after mean daily temperature exceeded 19.5–20.5°C, suggesting to us a threshold of around 20°C. Some limited evidence hints at a higher tolerance in extant populations (Cresswell 2004), including as high as 27°C for short times (Cramer and Hammack 1952:6), but we found no formal analyses of temperature-dependent mortality for adults holding in the Sacramento River system. At this writing (August 19, 2021), the holding adults in Butte Creek are undergoing another massive fish kill, reprising the events of 2002 and 2003: over 12,000 adults died between June 1 and July 27, 2021, concurrent with weeks of daily mean temperatures remaining between 20°C and 24°C (Cannon 2021).

Historic accounts claim that Chinook Salmon in the San Joaquin River system had unusually high thermal tolerance and were even prized as hatchery stocks for this reason (Yoshiyama et al. 2001). Even so, summer water temperatures evidently posed an ongoing struggle for existence: the Mariposa Gazette of August 26, 1882, reported

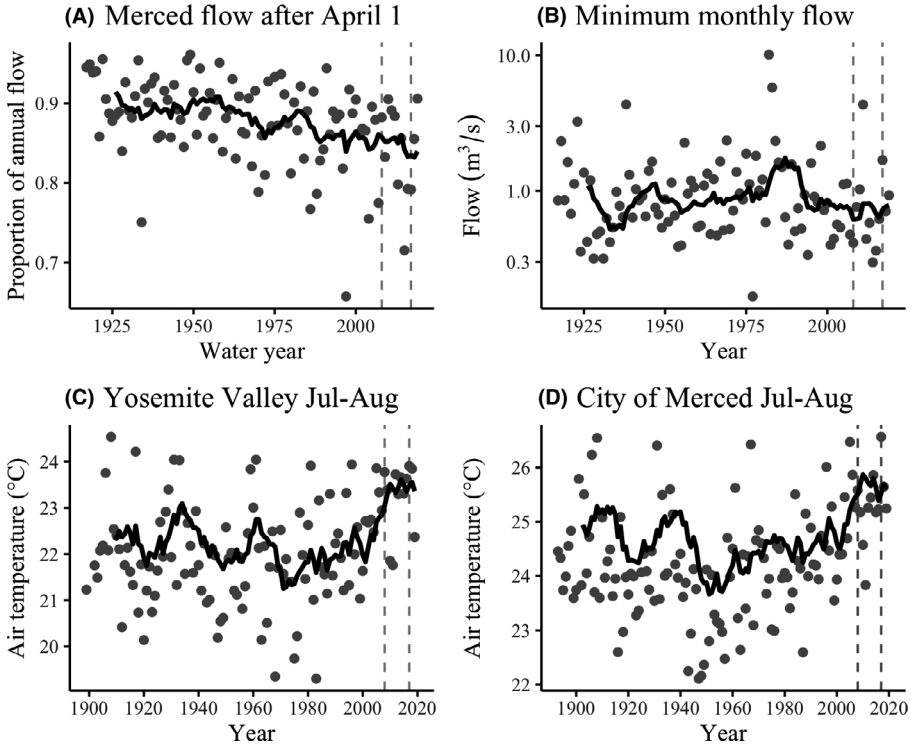

FIGURE 13. A century of river discharge and air temperature data from the Merced River region (dashed lines mark the decade examined in this paper; black lines mark the decadal running average): **(A)** proportion of annual discharge occurring on or after April 1 (approximate peak snowpack) of each water year for the Pohono Bridge gauge in the Yosemite Valley; **(B)** minimum monthly discharge during June–October at the Pohono Bridge gauge; **(C)** mean air temperature in the Yosemite Valley during July–August (U.S. Historical Climatology Network [USHCN] station USH00049855, elevation = 1,224.7 m, data set FLs.52i); and **(D)** mean air temperature near the City of Merced during July–August (USHCN station USH00045532, elevation = 46.6 m, data set FLs.52i).

TABLE 5. Deaths of adult spring-run Chinook Salmon while holding in Butte Creek, 2001–2003 (summarized from Ward et al. 2004).

				Highest daily temperature		
Year	Run size	Number of deaths	Holding mortality (%)	Daily maximum (°C)	Daily mean (°C)	Number of days on which mean > 20°C
2001	18,505	193	1	20.7	19.4	0
2002	16,328	3,431	21	22.3	20.8	5
2003	17,294	11,231	65	22.2	20.9	7

that "...the water in the Merced River has become so hot that it has caused all the salmon to die. Tons upon tons of dead fish are daily drifting down the river, which is creating a terrible stench..." (cited by Yoshiyama et al. 2001). This account likely came from the placer mining region now under McClure Reservoir, so we cannot say whether it reflects direct impacts of mining or fish drifting down from our reintroduction area, which was quite remote and undeveloped in 1882. However, it suggests that even 140 years ago, higher thermal tolerance was under strong natural selection. It is possible that substantial numbers of salmon could hold only in the cool years of the previous centuries and that those cool years have now become quite rare (Figure 13C, D).

Thermal tolerances for holding adults are better documented in the Pacific Northwest, where the climate is generally cooler but warm conditions are nevertheless common. There is little clear evidence for tolerances exceeding a daily mean temperature of 20°C or 21°C. Adult migration was blocked at 21–22°C in the Clearwater River (Idaho), Snake River, and Tucannon River, although possibly at slightly higher temperatures (23.9°C) in the Columbia River itself (Richter and Kolmes 2005 and references cited therein). In holding females, mortality and disease are common above 15.5°C (Richter and Kolmes 2005). In the Rogue River, wild spring-run Chinook Salmon suffered high prespawn mortality at temperatures ranging from 18°C to 21°C (McCullough 1999). In

tributaries of the Willamette River, Oregon, on average the prespawn mortality of mostly wild runs (15% hatchery origin) rose above 30% as the 7-d average of the *maximum* daily temperature exceeded 20°C (Bowerman et al. 2018); of course, the daily *mean* temperature associated with this mortality would have been substantially less than 20°C.

More broadly, Bowerman et al. (2021) found that spring-run Chinook Salmon adults in the mid- and upper Columbia River regions and spring-/summer-run adults in the Snake River region all suffered high levels of prespawn mortality in years when mean August temperature exceeded 18°C. In a regression model pooling data from throughout the Pacific Northwest, the prespawn mortality averaged about 50% as mean August temperature approached 20°C, but there was considerable scatter, suggesting important roles for environmental heterogeneity and local adaptation (Bowerman et al. 2021). Torgersen et al. (1999) observed some spring-run Chinook Salmon adults holding in temperatures as high as 23–25°C in the Middle Fork of the John Day River, Oregon, but these temperatures represented afternoon maximums rather than daily means, and in any case most adults disproportionately used cooler habitats.

Thus, it would have been unusual but not completely implausible for adults of the historic San Joaquin River populations to tolerate daily mean temperatures greater than 20°C over extended periods. Berman and Quinn (1991) found that holding adults in the Yakima River, Washington, could behaviorally thermoregulate to maintain body temperatures approximately 2.5°C cooler than ambient river temperatures over the range of 12.0–19.5°C. If adults of the extinct Merced River population had been able to maintain comparable differences at even higher temperatures, they might have been able to survive during most years, though with occasional fish kills as described in the Mariposa Gazette article of 1882. A key question is whether local adaptation could have evolved greater thermal tolerance than in other stocks versus a fundamental evolutionary constraint that puts a hard limit on tolerance, such as maximum cardiac output at high temperature (Farrell 2002). In our models, if we adjusted thermal tolerance upward, we found that the Merced River's holding capacity at the height of summer ballooned when the limit reached 23°C (Figure S.8). This suggests that if the San Joaquin River stocks historically had a thermal tolerance of 23°C rather than our assumed 20°C, the natural thermal regime of the upper Merced River would have supported good production.

Such production could only happen if the salmon also overcame thermal constraints on spawning. Our results suggested that spawning capacity in the Merced River system was quite low but could be much higher if Chinook Salmon either tolerated warmer conditions or spawned a month later. The assumed tolerance threshold for spawning was 14.4°C (after Bratovich et al. 2012), which is more restrictive than for holding to reflect that spawning is more metabolically demanding. This implicitly assumes a low metabolic scope for activity at high temperature, which occurs in some salmonid populations but not in those with a history of exposure to high water temperatures (Eliason et al. 2011; Verhille et al. 2016). In short, aerobic scope at high temperature responds to natural selection and can become adapted to local conditions, consistent with the historical accounts of thermally tolerant Chinook Salmon populations in San Joaquin River tributaries. Perhaps a reintroduced population with sufficient genetic variation could similarly adapt to the warm spawning conditions over time.

Alternatively, spawning capacity could expand if adults delayed their spawning until November, when conditions typically cooled down. We assumed a relatively compressed 6-week spawning season from mid-September to the end of October because Garman and McReynolds (2009) carefully documented as much in the Butte Creek population of spring-run Chinook Salmon. However, FitzGerald et al. (2020) recently reviewed accounts of spawn timing throughout California and found that spring-run Chinook Salmon may spawn as early as August or as late as December. Thompson et al. (2020) used whole-genome analysis to reject the hypothesis that this variation arose from local adaptation, and they gave evidence that it is better explained by the impact of temperature exposure on maturation rate. Since warmer temperature accelerates the maturation rate, the warm conditions in the Merced River would likely produce an early spawning season—opposite of what is needed—while the cooler conditions of the Tuolumne River would likely delay the spawning season, where it is not needed. Perhaps fully mature adults can delay the actual behavior of spawning until cued by suitable temperature; the answer likely depends on the interplay of direct physiological and behavioral response to temperature versus local adaptation to prevailing conditions (Beechie et al. 2008; see also the discussion by FitzGerald et al. 2020). Overall, the scope for local adaptation to the prevailing thermal regime seems greater for the spawning stage than for the holding stage.

Negative Spikes and Migratory Phenotypes

Our modeling produced negative spikes in fry capacity during winter storms and the snowmelt season, when high river discharge depressed the amount of shallow–slow habitat preferred by the fry of both species. Steelhead fry would be exposed to an extended dip from snowmelt, but they would typically emerge over an even longer window, so only a subset of the cohort would be exposed in any given year. Since the timing and magnitude of the "snowmelt dip" vary from year to year under a natural flow

regime (Figure 10, left column), this extended fry season should confer resilience to each cohort.

Chinook Salmon fry would be exposed to the sharp negative spikes that often occurred in January and February (Figure 9), potentially driving large numbers of fry downstream. Rutter (1904) may have been the first to document pulses of small, migrating fry moving downriver toward the Sacramento–San Joaquin Delta, in his case through the Sacramento River. Although he noted that "a large migration was not coincident with remarkably high water," he also described how fry migrated tail-first, swimming against the current and feeding as they go, thus reaching points along the river more slowly than the surrounding water. In fact, peak catches of fall-run fry in the Sacramento–San Joaquin Delta often follow major runoff periods, and higher fry abundances are observed during wet years (Kjelson and Raquel 1982; Brandes and McLain 2001).

Young Chinook Salmon exhibit a variety of migratory phenotypes (Miller and Gray 2010; Williams 2012; Sturrock et al. 2015; Munsch et al. 2019) involving both an initial life history decision of when to depart natal habitat and subsequent decisions about residence times in various low-gradient downstream habitats (Bourret and Caudill 2016). In extant spring-run populations in the Central Valley, most fry appear to move downstream shortly after emergence (Williams 2012), rearing quite successfully in low-gradient habitats on the valley floor (Cordoleani et al. 2018, 2019). On the other hand, fry that stay at high elevations and emigrate as yearlings can contribute disproportionately to adult runs, especially in drought years (Cordoleani et al. 2021).

In the Stanislaus River, a San Joaquin River tributary immediately north of the Tuolumne River, young *fall*-run Chinook Salmon may emigrate as fry, juveniles, subyearling smolts, or yearling smolts, but high proportions of emigrant fry or parr are associated with years of high cumulative flows (Zeug et al. 2014). Paradoxically, migrant fry are the most common phenotype but have the poorest survival to adulthood (Sturrock et al. 2020), although downstream rearing in floodplains, when available, may improve subsequent growth and survival (Zeug et al. 2019), and years of high flow also support greater survival (Zeug et al. 2020). The negative spikes in capacity observed during our study suggest that perhaps the initial life history decision of spring-run Chinook Salmon emerging from the gravel is not so much whether to go but how to stay. Those fry that manage to find velocity refuges and stay in the mountains would presumably enjoy a low level of competition between storms. Those that are driven downstream could locate high-reward feeding habitat, such as valley floodplains or the estuary if not blocked by reservoirs, levees, or channel incision (Sellheim et al. 2016; Zeug et al. 2019). However, the risk of predation is also high and contingent on flow patterns (Lindley et al. 2009; Michel 2019; Sturrock et al. 2020).

Steelhead fry that are not driven downstream by snowmelt would presumably shift their hydraulic niche as they grow into juveniles: from slow water at a variety of depths to shallow water at a variety of velocities (Figure 6). This finding supports McEwan's (2001) view that steelhead fry are generally velocity limited but specialize on swifter water as they grow.

Making Salmon in the Anthropocene

Our results suggest that steelhead reintroduction could succeed in either system and that Chinook Salmon could succeed in the Tuolumne River due to its tighter thermal buffering. The Merced River appeared to be too warm for adult Chinook Salmon to hold through the dry season, but existing stocks from the Sacramento River system seem to have a lower thermal tolerance than the extinct San Joaquin River stocks. In fact, the thermal tolerance of holding adults is poorly characterized for Central Valley populations and deserves better study given its importance for successful reintroduction. More extensive work on thermal tolerances in the Pacific Northwest suggests that San Joaquin River populations would have been outliers but plausibly within the scope for local adaptation, and the historical record suggests that thermal fish kills happened even in the 19th century, but cool years were also much more frequent than in recent decades. The prospects for successful reintroduction of spring-run Chinook Salmon are therefore much more ambiguous for the Merced River than for the Tuolumne River, where recent operations of the Hetch Hetchy System produce a large thermal refugium sustained by passive thermal buffering of streamflows. This thermal refugium has a promising capacity for holding adults, spawning adults, and the yearling life history type that plays an important role in drought resilience.

Thus, the quandaries of "making salmon" in the Anthropocene. In his book *Making Salmon: An Environmental History of the Northwest Fisheries Crisis*, Taylor (1999) showed that while many different actors spoke out on behalf of salmon conservation during the 20th century, they in fact tended to articulate their own desires rather than the needs of the salmon; Taylor (1999) also demonstrated that science and scientists tended to aid and abet this process, creating a "durable crisis." Although the mix of mitigation measures may have changed since 1999, what about the underlying durable crisis? In the most recently completed status review of spring-run Chinook Salmon in the Central Valley (Williams et al. 2016), only 4 of the 18 or 19 original independent populations were still extant and only one (Butte Creek) was at low risk of extinction. As mentioned above, the large recent run of adults in Butte Creek is undergoing a massive fish kill (>12,000 dead) associated with high water temperatures

during the holding phase (Cannon 2021). Hence, the durable crisis appears to remain durable.

The upper Tuolumne River represents an immediate opportunity to create a sustainable population—perhaps larger than any extant population of spring-run Chinook Salmon in the Central Valley—by using existing spring-run stocks and a passive thermal buffering system that is already in operation. Of course, this thermal buffering system also generates hydroelectricity in an era when electric power supplies need to rapidly decarbonize, but it also happens to embody a potent symbol as the catalyst for modern political environmentalism (Righter 2005), and any effort to use the Hetch Hetchy System to establish a new, resilient salmon population will likely become entangled with this symbolism in complicated ways.

Perhaps the emphasis should instead be on reintroduction into the Merced River, a more truly wild river but one in which success appears to rely on the evolution—or re-evolution—of a "new" wild fish with new thermal tolerances to replace the extinct stocks that were subject to thermal fish kills even 140 years ago, prior to most effects of anthropogenic climate change. If we factor in a forward-looking time scale of 100 years, as is conventional for the conservation of endangered species (Soulé 1987; McElhany et al. 2000), the limits posed by climate change seem even clearer. Such are the decisions that increasingly play out in the Anthropocene, a 70-year-old geologic era characterized not by the brief presence of modern human beings but by our permanent deflection of the course of evolutionary change on Earth at geologic time scales (Brannen 2019). The Anthropocene

> doesn't stake out a hopeful future and it doesn't stake out a catastrophic future... It just says that if you want to be a sentient species you have to reckon with the degree to which you have already changed things... If you back away from that obligation you're not being a better scientist; you're being a worse scientist [S. Wing, quoted by Brannen 2019].That reckoning suggests that going forward, the passive thermal buffering of the Tuolumne River represents an unusual—perhaps unique—opportunity to establish a sustainable, climate-resilient population of spring-run Chinook Salmon in the Central Valley of California.

The recipe to "make" either salmon or steelhead in the upper Tuolumne River, however, requires additional ingredients. One significant challenge is the recent poor survival of smolts migrating through the San Joaquin Delta and San Joaquin River (Buchanan et al. 2013, 2018), although these studies have tended to focus on movements in April and May, when survival tends to be lowest (Sturrock et al. 2020). Fry would emigrate sooner, and in the fall run of Chinook Salmon, emigrant fry are so abundant that even a modest improvement in their recent survival would likely have a large effect on adult abundance (Sturrock et al. 2020). Our results suggest that for a reintroduced spring run to the now inaccessible Tuolumne or Merced rivers, winter storms would likewise drive large numbers of fry downstream and the success of reintroduction would hinge on their fate. For steelhead, snowmelt would do the same a few months later.

Thus, one key ingredient for reintroduction is a downstream passage strategy that encompasses migrant fry, parr, and smolts of both species at high enough collection rates to support self-sustaining populations. Anchor QEA (2017) outlined the design of a hybrid fish collector for the head of the Don Pedro Reservoir on Tuolumne River that would meet this need, collecting 100% of emigrants up to discharges of 120 m^3/s, thereafter declining with discharge to about 75% at 170 m^3/s, although some improvement may be possible through adaptive management of guidance curtains. This solution, however, requires construction of a new low-head dam at the head of the reservoir to fortify the hybrid collector.

If built, the hybrid fish collector would be expected to generate an annual supply of captured emigrant fry, parr, and smolts of both species to be hauled to some set of release points downstream of the dams. Mortality of released emigrants is expected to be high in the lower Tuolumne River (Sonke 2020; Zeug et al. 2020), the lower San Joaquin River (Michel et al. 2018), and the San Joaquin River Delta (Buchanan et al. 2013, 2018; Perry et al. 2016), but growth and survival would likely be improved for fish that are able to access inundated floodplain habitats (Sommer et al. 2001; Jeffres et al. 2008; Opperman et al. 2010; Zeug et al. 2019). Thus, the success of reintroduction is likely to be sensitive to (1) the exact strategy for when and where to release emigrants and (2) ongoing efforts to restore floodplain habitats that are accessible to the released emigrants. Perhaps some emigrants could be released directly into restored floodplain habitat, such as the Dos Rios Preserve at the confluence of the Tuolumne and San Joaquin rivers (Duggan 2021). Clearly, the next step is to design and examine a variety of quantitative scenarios for reintroduction that account for survival and life history diversity over the entire life cycle of the fish, across a realistic diversity of management strategies and climatic constraints, to answer the question: What is the most promising strategy for establishing sustainable populations of these two anadromous fishes to the central Sierra Nevada, where the combination of high elevation and the Hetch Hetchy System appears to generate a resilient thermal refugium during an era of rapidly warming climate?

ACKNOWLEDGMENTS

We thank John Wooster for many insights on these rivers, river rangers of the Bureau of Land Management's

Mother Lode Field Office and the Sierra National Forest for transporting us through the study reaches, and Ian Bell for technical assistance in the field. Mark Gard kindly shared original data from Yuba River studies. Andrew Pike helped in many tangible and intangible ways. Peter Dudley, Alyssa FitzGerald, Nate Mantua, George Pess, and one anonymous reviewer read the manuscript and provided thoughtful and helpful comments. There is no conflict of interest declared in this article.

ORCID

David A. Boughton https://orcid.org/0000-0002-5843-6494
Lee R. Harrison https://orcid.org/0000-0002-5219-9280
Sara N. John https://orcid.org/0000-0002-3761-4722
Rosealea M. Bond https://orcid.org/0000-0003-0939-2007
Colin L. Nicol https://orcid.org/0000-0003-1080-323X
Carl J. Legleiter https://orcid.org/0000-0003-0940-8013
Ryan T. Richardson https://orcid.org/0000-0002-7864-8670

REFERENCES

Agrawal, A., R. S. Schick, E. P. Bjorkstedt, R. G. Szerlong, M. N. Goslin, B. Spence, T. H. Williams, and K. M. Burnett. 2005. Predicting the potential for historical Coho, Chinook and steelhead habitat in northern California. NOAA Technical Memorandum NMFS-SWFSC-379.

Anchor QEA. 2017. Conceptual engineering plans for fish passage at La Grange and Don Pedro dams on the Tuolumne River. Prepared for National Oceanic and Atmospheric Administration Fisheries, California Central Valley Office, Sacramento.

Anderson, J. H., G. R. Pess, P. M. Kiffney, T. R. Bennett, P. L. Faulds, W. I. Atlas, and T. P. Quinn. 2013. Dispersal and tributary immigration by juvenile Coho Salmon contribute to spatial expansion during colonisation. Ecology of Freshwater Fish 22:30–42.

Ayllon, D., A. Almodovar, G. G. Nicola, I. Parra, and B. Elvira. 2012. Modelling carrying capacity dynamics for the conservation and management of territorial salmonids. Fisheries Research 134:95–103.

Ballard, E., M. Gard, and B. Pelle. 2010a. Flow–habitat relationships for juvenile fall/spring-run Chinook Salmon and steelhead/Rainbow Trout rearing in the Yuba River. U.S. Fish and Wildlife Service, Sacramento Fish and Wildlife Office, Sacramento, California.

Ballard, E., M. Gard, and B. Pelle. 2010b. Flow–habitat relationships for spring and fall-run Chinook Salmon and steelhead/Rainbow Trout spawning in the Yuba River. U.S. Fish and Wildlife Service, Sacramento Fish and Wildlife Office, Sacramento, California.

Beechie, T., E. Buhle, M. Ruckelshaus, A. Fullerton, and L. Holsinger. 2006. Hydrologic regime and the conservation of salmon life history diversity. Biological Conservation 130:560–572.

Beechie, T., H. Moir, and G. Pess. 2008. Hierarchical physical controls on salmonid spawning location and timing. Pages 83–101 *in* D. A. Sear and P. DeVries, editors. Salmonid spawning habitat in rivers: physical controls, biological responses, and approaches to remediation. American Fisheries Society, Symposium 65, Bethesda, Maryland.

Benjankar, R. M., D. Tonina, J. A. McKean, M. M. Sohrabi, Q. Chen, and D. Vidergar. 2018. Dam operations may improve aquatic habitat and offset negative effects of climate change. Journal of Environmental Management 213:126–134.

Berman, C. H., and T. P. Quinn. 1991. Behavioral thermoregulation and homing by spring Chinook Salmon, *Oncorhynchus tshawytscha* (Walbaum), in the Yakima River. Journal of Fish Biology 39:301–312.

Bjorkstedt, E. P., B. C. Spence, J. C. Garza, D. G. Hankin, D. Fuller, W. E. Jones, J. J. Smith, and R. Macedo. 2005. An analysis of historical population structure for evolutionarily significant units of Chinook Salmon, Coho Salmon, and steelhead in the north-central California coast recovery domain. NOAA Technical Memorandum NMFS-SWFSC-382.

Bouchard, C., A. Bardonnet, M. Buoro, and C. Tentelier. 2018. Effects of spatial aggregation of nests on population recruitment: the case of a small population of Atlantic Salmon. Ecosphere [online serial] 9(4): e02178.

Bourret, S. L., C. C. Caudill, and M. L. Keefer. 2016. Diversity of juvenile Chinook Salmon life history pathways. Reviews in Fish Biology and Fisheries 26:375–403.

Bowerman, T. E., M. L. Keefer, and C. C. Caudill. 2021. Elevated stream temperature, origin, and individual size influence Chinook Salmon prespawn mortality across the Columbia River basin. Fisheries Research 237:105874.

Bowerman, T., A. Roumasset, M. L. Keefer, C. S. Sharpe, and C. C. Caudill. 2018. Prespawn mortality of female Chinook Salmon increases with water temperature and percent hatchery origin. Transactions of the American Fisheries Society 147:31–42.

Braithwaite, J. E., J. J. Meeuwig, and K. C. S. Jenner. 2012. Estimating cetacean carrying capacity based on spacing behaviour. PLOS (Public Library of Science) ONE [online serial] 7(12):e51347.

Brandes, P. L., and J. S. McLain. 2001. Juvenile Chinook Salmon abundance, distribution, and survival in the Sacramento–San Joaquin Estuary. California Department of Fish and Game Fish Bulletin 179:39–138.

Brannen, P. 2019. What made me reconsider the Anthropocene. The Atlantic (October 11).

Bratovich, P., C. Addley, D. Simodynes, and H. Bowen, 2012. Water temperature considerations for Yuba River basin anadromous salmonid reintroduction evaluations. Yuba Salmon Forum Technical Working Group, Sacramento, California.

Brunner, G. W. 2010. HEC-RAS River Analysis System hydraulic reference manual. Hydrologic Engineering Center, Davis, California.

Buchanan, R. A., P. L. Brandes, and J. R. Skalski. 2018. Survival of juvenile fall-run Chinook Salmon through the San Joaquin River Delta, California, 2010–2015. North American Journal of Fisheries Management 38:663–679.

Buchanan, R. A., J. R. Skalski, P. L. Brandes, and A. Fuller. 2013. Route use and survival of juvenile Chinook Salmon through the San Joaquin River Delta. North American Journal of Fisheries Management 33:216–229.

Buffington, J. M., D. R. Montgomery, and H. M. Greenberg. 2004. Basin-scale availability of salmonid spawning gravel as influenced by channel type and hydraulic roughness in mountain catchments. Canadian Journal of Fisheries and Aquatic Sciences 61:2085–2096.

Burnett, K. M., G. H. Reeves, D. J. Miller, S. Clarke, K. Vance-Borland, and K. Christiansen. 2007. Distribution of salmon-habitat potential relative to landscape characteristics and implications for conservation. Ecological Applications 17:66–80.

Burnham, K. P., and D. R. Anderson. 2002. Model selection and multimodel inference: a practical information-theoretic approach, 2nd edition. Springer-Verlag, New York.

Busby, P. J., T. C. Wainwright, G. J. Bryant, L. Lierheimer, R. S. Waples, F. W. Waknitz, and I. V. Lagomarsino. 1996. Status review of West Coast steelhead from Washington, Idaho, Oregon, and California. NOAA Technical Memorandum NMFS-NWFSC-27.

Cain, J., J. Ferguson, E. Appy, J. Rosenfeld, A. Weber-Stover, S. Louie, J. Shelton, T. Heyne, A. Fuller, B. Ellrott, S. Franks, M. Gutierrez, R. Reed, D. R. Swank, S. Edmundson, R. Johnson, J. Howard, C. Carr, D. Worth, R. Henery, R. Yoshiyama, J. Israel, P. Cadrett, R. Martin, J. D. Wikert, and J. Zimmerman. 2015. Interim objectives for restoring Chinook Salmon (*Oncorhynchus tshawytscha*) and *O. mykiss* in the Stanislaus River. Anchor QEA, Seattle, Washington.

Cannon, T. 2021. Butte Creek spring-run Chinook Salmon in peril. California Fisheries Blog (California Sportfishing Protection Alliance) (August 4).

Carbonneau, P., M. A. Fonstad, W. A. Marcus, and S. J. Dugdale. 2012. Making riverscapes real. Geomorphology 137:74–86.

Chapman, D. W. 1966. Food and space as regulators of salmonid populations in streams. American Naturalist 100:345–357.

Chapman, E. J., and C. J. Byron. 2018. The flexible application of carrying capacity in ecology. Global Ecology and Conservation [online serial] 13:e00365.

Cooper, E. J., A. P. O'Dowd, J. J. Graham, D. W. Mierau, W. J. Trush, and R. Taylor. 2020. Salmonid habitat and population capacity estimates for steelhead trout and Chinook Salmon upstream of Scott Dam in the Eel River, California. Northwest Science 94:70–96.

Cordoleani, F., J. Notch, A. S. McHuron, A. J. Ammann, and C. J. Michel. 2018. Movement and survival of wild Chinook Salmon smolts from Butte Creek during their out-migration to the ocean: comparison of a dry year versus a wet year. Transactions of the American Fisheries Society 147:171–184.

Cordoleani, F., J. Notch, A. S. McHuron, C. Michel, and A. J. Ammann. 2019. Movement and survival rates of Butte Creek spring-run Chinook Salmon smolts from the Sutter Bypass to the Golden Gate Bridge in 2015, 2016, and 2017. NOAA Technical Memorandum NMFS-SWFSC-618.

Cordoleani, F., C. C. Phillis, A. M. Sturrock, A. M. FitzGerald, A. Malkassian, G. E. Whitman, P. K. Weber, and R. C. Johnson. 2021. Threatened salmon rely on a rare life history strategy in a warming landscape. Nature Climate Change 11:982–988.

Cramer, F. K., and D. F. Hammack. 1952. Salmon research at Deer Creek, Calif. U.S. Fish and Wildlife Service Special Scientific Report Fisheries 67.

Cresswell, D. J. 2004. Summer stream temperatures experienced by adult spring-run Chinook Salmon (*Oncorhynchus tshawytscha*) in a Central Valley stream. Master's thesis. California State University, Chico.

del Monte-Luna, P., B. W. Brook, M. J. Zetina-Rejon, and V. H. Cruz-Escalona. 2004. The carrying capacity of ecosystems. Global Ecology and Biogeography 13:485–495.

Duggan, T. 2021. Could this $36 million Central Valley river restoration project help with California's droughts? San Francisco Chronicle (May 10).

Ebersole, J. L., W. J. Liss, and C. A. Frissell. 2003. Thermal heterogeneity, stream channel morphology, and salmonid abundance in northeastern Oregon streams. Canadian Journal of Fisheries and Aquatic Sciences 60:1266–1280.

Einum, S., L. Sundt-Hansen, and K. H. Nislow. 2006. The partitioning of density-dependent dispersal, growth and survival throughout ontogeny in a highly fecund organism. Oikos 113:489–496.

Eliason, E. J., T. D. Clark, M. J. Hague, L. M. Hanson, Z. S. Gallagher, K. M. Jeffries, M. K. Gale, D. A. Patterson, S. G. Hinch, and A. P. Farrell. 2011. Differences in thermal tolerance among Sockeye Salmon populations. Science 332:109–112.

Falcy, M. R. 2015. Density-dependent habitat selection of spawning Chinook Salmon: broad-scale evidence and implications. Journal of Animal Ecology 84:545–553.

Farrell, A. R. 2002. Cardiorespiratory performance in salmonids during exercise at high temperature: insights into cardiovascular design limitations in fishes. Comparative Biochemistry and Physiology Part A: Molecular and Integrative Physiology 132:797–810.

Fausch, K. D., C. E. Torgersen, C. V. Baxter, and H. W. Li. 2002. Landscapes to riverscapes: bridging the gap between research and conservation of stream fishes. BioScience 52:483–498.

FitzGerald, A. M., S. N. John, T. M. Apgar, N. J. Mantua, and B. T. Martin. 2020. Quantifying thermal exposure for migratory riverine species: phenology of Chinook Salmon populations predicts thermal stress. Global Change Biology 27:536–549.

Garman, C. E., and T. R. McReynolds. 2009. Butte and Big Chico creeks, spring-run Chinook Salmon, *Oncorhynchus tshawytscha* life history investigation, 2007–2008. California Department of Fish and Wildlife, Rancho Cordova.

Golyandina, N., and A. Korobeynikov. 2014. Basic singular spectrum analysis and forecasting with R. Computational Statistics and Data Analysis 71:934–954.

Grant, J. W. A., and D. L. Kramer. 1990. Territory size as a predictor of the upper limit to population-density of juvenile salmonids in streams. Canadian Journal of Fisheries and Aquatic Sciences 47:1724–1737.

Greene, C. M., and T. J. Beechie. 2004. Consequences of potential density-dependent mechanisms on recovery of ocean-type Chinook Salmon (*Oncorhynchus tshawytscha*). Canadian Journal of Fisheries and Aquatic Sciences 61:590–602.

Hanson, W. D., F. Kukula, C. Nelson, and M. Williams. 2005. San Francisco water and power: a history of the Municipal Water Department and Hetch Hetchy System. San Francisco Public Utilities Commission, San Francisco.

Harrison, L. R., A. Pike, and D. A. Boughton. 2017. Coupled geomorphic and habitat response to a flood pulse revealed by remote sensing. Ecohydrology [online serial] 10(5):e1845.

Hosmer, D. W. Jr., S. Lemeshow, and R. X. Sturdivant. 2013. Applied logistic regression, 3rd edition. Wiley, Hoboken, New Jersey.

Hugue, F., M. Lapointe, B. C. Eaton, and A. Lepoutre. 2016. Satellite-based remote sensing of running water habitats at large riverscape scales: tools to analyze habitat heterogeneity for river ecosystem management. Geomorphology 253:353–369.

Huntsman, B. M., J. A. Falke, J. W. Savereide, and K. E. Bennett. 2017. The role of density-dependent and -independent processes in spawning habitat selection by salmon in an Arctic riverscape. PLOS (Public Library of Science) ONE [online serial] 12(5):e0177467.

Imre, I., J. W. A. Grant, and E. R. Keeley. 2004. The effect of food abundance on territory size and population density of juvenile steelhead trout (*Oncorhynchus mykiss*). Oecologia 138:371–378.

Jeffres, C. A., J. J. Opperman, and P. B. Moyle. 2008. Ephemeral floodplain habitats provide best growth conditions for juvenile Chinook Salmon in a California river. Environmental Biology of Fishes 83:449–458.

Kannry, S. H., S. M. O'Rourke, S. J. Kelson, and M. R. Miller. 2020. On the ecology and distribution of steelhead (*Oncorhynchus mykiss*) in California's Eel River. Journal of Heredity 111:548–563.

Kjelson, M. A., P. F. Raquel, and F. W. Fisher. 1982. Life history of fall-run juvenile Chinook Salmon, *Oncorhynchus tshawytscha*, in the Sacramento–San Joaquin Estuary, California. Pages 393–411 *in* V. S. Kennedy, editor. Estuarine comparisons. Academic Press, New York.

Kock, T. J., J. W. Ferguson, M. L. Keefer, and C. B. Schreck. 2021. Review of trap-and-haul for managing Pacific salmonids (*Oncorhynchus* spp.) in impounded river systems. Reviews in Fish Biology and Fisheries 31:53–94.

Kock, T. J., N. E. Verretto, N. K. Ackerman, R. W. Perry, J. W. Beeman, M. C. Garello, and S. D. Fielding. 2019. Assessment of operational and structural factors influencing performance of fish collectors in forebays of high-head dams. Transactions of the American Fisheries Society 148:464–479.

Kondolf, G. M. 1997. Hungry water: effects of dams and gravel mining on river channels. Environmental Management 21:533–551.

Koschmann, A. H., and M. H. Bergendahl. 1968. Principal gold-producing districts of the United States. U.S. Geological Survey Professional Paper 610.

Lang, H. O. 1882. A history of Tuolumne County, California. B. F. Alley, San Francisco.

Lee, D. P. 2020. California winter steelhead: life history and fly fishing. Gardull Graphics, Folsom, California.

Legleiter, C. J. 2012. Remote measurement of river morphology via fusion of LiDAR topography and spectrally based bathymetry. Earth Surface Processes and Landforms 37:499–518.

Legleiter, C. J., and R. L. Fosness. 2019. Defining the limits of spectrally based bathymetric mapping on a large river. Remote Sensing [online serial] 11(6):article 665.

Legleiter, C. J., and L. R. Harrison. 2019. Remote sensing of river bathymetry: evaluating a range of sensors, platforms, and algorithms on the upper Sacramento River, California, USA. Water Resources Research 55:2142–2169.

Legleiter, C. J., L. R. Harrison, D. A. Boughton, C. M. Nicol, and R. R. Richardson. 2020. Topographic and sediment grain size data used to evaluate potential habitat for anadromous salmonids on the upper Merced and Tuolumne rivers in California. U.S. Geological Survey, Data Release, Reston, Virginia. Available: https://doi.org/10.5066/P9MUPT5X. (November 2020).

Legleiter, C. J., B. T. Overstreet, and P. J. Kinzel. 2018. Sampling strategies to improve passive optical remote sensing of river bathymetry. Remote Sensing [online serial] 10(6):article 935.

Legleiter, C. J., D. A. Roberts, and R. L. Lawrence. 2009. Spectrally based remote sensing of river bathymetry. Earth Surface Processes and Landforms 34:1039–1059.

Leitwein, M., J. C. Garza, and D. E. Pearse. 2017. Ancestry and adaptive evolution of anadromous, resident, and adfluvial Rainbow Trout (*Oncorhynchus mykiss*) in the San Francisco Bay area: application of adaptive genomic variation to conservation in a highly impacted landscape. Evolutionary Applications 10:56–67.

Leopold, A. 1933. Game management. Scribner, New York.

Lindley, S. T., C. B. Grimes, M. S. Mohr, W. Peterson, J. Stein, J. T. Anderson, L. W. Botsford, D. L. Bottom, C. A. Busack, T. K. Collier, J. Ferguson, J. C. Garza, A. M. Grover, D. G. Hankin, R. G. Kope, P. W. Lawson, A. Low, R. B. MacFarlane, K. Moore, M. Palmer-Zwahlen, F. B. Schwing, J. Smith, C. Tracy, R. Webb, B. K. Wells, and T. H. Williams. 2009. What caused the Sacramento River fall Chinook stock collapse? NOAA Technical Memorandum NMFS-SWFSC-447.

Lindley, S. T., R. S. Schick, E. Mora, P. B. Adams, J. J. Anderson, S. Greene, C. Hanson, B. P. May, D. R. McEwan, R. B. MacFarlane, C. Swanson, and J. G. Williams. 2007. Framework for assessing viability of threatened and endangered Chinook Salmon and steelhead in the Sacramento–San Joaquin basin. San Francisco Estuary and Watershed Science [online serial] 5(1):article 4.

Lusardi, R. A., and P. B. Moyle. 2017. Two-way trap and haul as a conservation strategy for anadromous salmonids. Fisheries 42:478–487.

Matthews, K. R., and N. H. Berg. 1997. Rainbow Trout responses to water temperature and dissolved oxygen stress in two southern California stream pools. Journal of Fish Biology 50:50–67.

McClure, M. M., S. M. Carlson, T. J. Beechie, G. R. Pess, J. C. Jorgensen, S. M. Sogard, S. E. Sultan, D. M. Holzer, J. Travis, B. L. Sanderson, M. E. Power, and R. W. Carmichael. 2008. Evolutionary consequences of habitat loss for Pacific anadromous salmonids. Evolutionary Applications 1:300–318.

McCullough, D. A. 1999. A review and synthesis of effects of alterations to the water temperature regime on freshwater life stages of salmonids, with special reference to Chinook Salmon. Columbia River Inter-Tribal Fish Commission, Portland, Oregon.

McElhany, P., M. H. Ruckelshaus, M. J. Ford, T. C. Wainwright, and E. P. Bjorkstedt. 2000. Viable salmonid populations and the recovery of evolutionarily significant units. NOAA Technical Memorandum NMFS-SWFSC-42.

McEwan, D. R. 2001. Central Valley steelhead. California Department of Fish and Game Fish Bulletin 179:1–79.

McHugh, P. A., W. C. Saunders, N. Bouwes, C. E. Wall, S. Bangen, J. M. Wheaton, M. Nahorniak, J. R. Ruzycki, I. A. Tattam, and C. E. Jordon. 2017. Linking models across scales to assess the viability and restoration potential of a threatened population of steelhead (*Oncorhynchus mykiss*) in the Middle Fork John Day River, Oregon, USA. Ecological Modelling 355:24–38.

McLeod, S. R. 1997. Is the concept of carrying capacity useful in variable environments? Oikos 79:529–542.

Michel, C. J. 2019. Decoupling outmigration from marine survival indicates outsized influence of streamflow on cohort success for California's Chinook Salmon populations. Canadian Journal of Fisheries and Aquatic Sciences 76:1398–1410.

Michel, C. J., J. M. Smith, N. J. Demetras, D. D. Huff, and S. A. Hayes. 2018. Non-native fish predator density and molecular-based diet estimates suggest differing effects of predator species on juvenile salmon in San Joaquin River, California. San Francisco Estuary and Watershed Science [online serial] 16(4):article 3.

Miller, J. A., A. Gray, and J. Merz. 2010. Quantifying the contribution of juvenile migratory phenotypes in a population of Chinook Salmon *Oncorhynchus tshawytscha*. Marine Ecology Progress Series 408:227–240.

Mitchell, K. E., D. Lohmann, P. R. Houser, E. F. Wood, J. C. Schaake, A. Robock, B. A. Cosgrove, J. Sheffield, Q. Y. Duan, L. F. Luo, R. W. Higgins, R. T. Pinker, J. D. Tarpley, D. P. Lettenmaier, C. H. Marshall, J. K. Entin, M. Pan, W. Shi, V. Koren, J. Meng, B. H. Ramsay, and A. A. Bailey. 2004. The multi-institution North American Land Data Assimilation System (NLDAS): utilizing multiple GCIP products and partners in a continental distributed hydrological modeling system. Journal of Geophysical Research: Atmospheres [online serial] 109(D07S90).

Mobrand, L. E., J. A. Lichatowich, L. C. Lestelle, and T. S. Vogel. 1997. An approach to describing ecosystem performance "through the eyes of salmon." Canadian Journal of Fisheries and Aquatic Sciences 54:2964–2973.

Moir, H. J., and G. B. Pasternack. 2008. Relationships between mesoscale morphological units, stream hydraulics and Chinook Salmon (*Oncorhynchus tshawytscha*) spawning habitat on the lower Yuba River, California. Geomorphology 100:527–548.

Montgomery, D. R., and J. M. Buffington. 1997. Channel-reach morphology in mountain drainage basins. Geological Society of America Bulletin 109:596–611.

Moyle, P. B. 2002. Inland fishes of California. University of California Press, Berkeley.

Munsch, S. H., C. M. Greene, R. C. Johnson, W. H. Satterthwaite, H. Imaki, and P. L. Brandes. 2019. Warm, dry winters truncate timing and size distribution of seaward-migrating salmon across a large, regulated watershed. Ecological Applications [online serial] 29(4):e01880.

Nakamoto, R. J. 1994. Characteristics of pools used by adult summer steelhead oversummering in the New River, California. Transactions of the American Fisheries Society 123:757–765.

Needham, P. R., O. R. Smith, and H. A. Hanson. 1941. Salmon salvage problems in relation to Shasta Dam, California, and notes on the biology of Sacramento River salmon. Transactions of the American Fisheries Society 70:55–69.

Nickelson, T. E., J. D. Rodgers, S. L. Johnson, and M. F. Solazzi. 1992. Seasonal-changes in habitat use by juvenile Coho Salmon

(*Oncorhynchus kisutch*) in Oregon coastal streams. Canadian Journal of Fisheries and Aquatic Sciences 49:783–789.

Nielsen, J. L., T. E. Lisle, and V. Ozaki. 1994. Thermally stratified pools and their use by steelhead in northern California streams. Transactions of the American Fisheries Society 123:613–626.

Null, S. E., J. H. Viers, and J. F. Mount. 2010. Hydrologic response and watershed sensitivity to climate warming in California's Sierra Nevada. PLOS (Public Library of Science) ONE [online serial] 5(3): e9932.

O'Donnell, D., A. Rushworth, A. W. Bowman, E. M. Scott, and M. Hallard. 2014. Flexible regression models over river networks. Journal of the Royal Statistical Society Series C: Applied Statistics 63:47–63.

O'Neil, S. T., K. C. Rahn, and J. K. Bump. 2014. Habitat capacity for cougar recolonization in the upper Great Lakes region. PLOS (Public Library of Science) ONE [online serial] 9(11):e112565.

Opperman, J. J., R. Luster, B. A. McKenney, M. Roberts, and A. W. Meadows. 2010. Ecologically functional floodplains: connectivity, flow regime, and scale. Journal of the American Water Resources Association 46:211–226.

Passalacqua, P., P. Belmont, D. M. Staley, J. D. Simley, J. R. Arrowsmith, C. A. Bode, C. Crosby, S. B. DeLong, N. F. Glenn, S. A. Kelly, D. Lague, H. Sangireddy, K. Schaffrath, D. G. Tarboton, T. Wasklewicz, and J. M. Wheaton. 2015. Analyzing high resolution topography for advancing the understanding of mass and energy transfer through landscapes: a review. Earth-Science Reviews 148:174–193.

Pearse, D. E., and M. A. Campbell. 2018. Ancestry and adaptation of Rainbow Trout in Yosemite National Park. Fisheries 43:472–484.

Perkins, L. B., and A. J. Leffler. 2018. Conceptualizing ecological restoration: a concise and adaptable framework for researchers and practitioners. Restoration Ecology 26:1024–1028.

Perry, R. W., R. A. Buchanan, P. L. Brandes, J. R. Burau, and J. Israel. 2016. Anadromous salmonids in the Delta: new science 2006–2016. San Francisco Estuary and Watershed Science [online serial] 14 (2):2006–2016.

Peterson, E. E., and J. M. Ver Hoef. 2014. STARS: an ArcGIS toolset used to calculate the spatial information needed to fit spatial statistical models to stream network data. Journal of Statistical Software [online serial] 56(2).

Pfeiffer, A. M., and N. J. Finnegan. 2017. Basin-scale methods for predicting salmonid spawning habitat via grain size and riffle spacing, tested in a California coastal drainage. Earth Surface Processes and Landforms 42:941–955.

Pike, A., E. Danner, D. Boughton, F. Melton, R. Nemani, B. Rajagopalan, and S. Lindley. 2013. Forecasting river temperatures in real time using a stochastic dynamics approach. Water Resources Research 49:5168–5182.

Railsback, S. F. 2016. Why it is time to put PHABSIM out to pasture. Fisheries 41:720–725.

Richardson, R. T. 2016. Expanding fluvial remote sensing to the riverscape: mapping depth and grain size on the Merced River, California. Master's thesis. University of Wyoming, Laramie.

Richter, A., and S. A. Kolmes. 2005. Maximum temperature limits for Chinook, Coho, and Chum salmon, and steelhead trout in the Pacific Northwest. Reviews in Fisheries Science 13:23–49.

Riebe, C. S., L. S. Sklar, B. T. Overstreet, and J. K. Wooster. 2014. Optimal reproduction in salmon spawning substrates linked to grain size and fish length. Water Resources Research 50:898–918.

Righter, R. 2005. The battle over Hetch Hetchy: America's most controversial dam and the birth of modern environmentalism. Oxford University Press, New York.

Rosenfeld, J. S. 2014. Modelling the effects of habitat on self-thinning, energy equivalence, and optimal habitat structure for juvenile trout. Canadian Journal of Fisheries and Aquatic Sciences 71:1395–1406.

Rushworth, A. 2017. smnet: smoothing for stream network data. R package version 2.1.1. Available: https://CRAN.R-project.org/package=smnet. (December 2017).

Rutter, C. 1904. Natural history of the Quinnat Salmon. A report of investigations in the Sacramento River, 1896–1901. Bulletin of the U.S. Fish Commission 22:65–142.

Sayre, N. F. 2008. The genesis, history, and limits of carrying capacity. Annals of the Association of American Geographers 98:120–134.

Sellheim, K. L., C. B. Watry, B. Rook, S. C. Zeug, J. Hannon, J. Zimmerman, K. Dove, and J. E. Merz. 2016. Juvenile salmonid utilization of floodplain rearing habitat after gravel augmentation in a regulated river. River Research and Applications 32:610–621.

Sergeant, C. J., J. R. Bellmore, C. McConnell, and J. W. Moore. 2017. High salmon density and low discharge create periodic hypoxia in coastal rivers. Ecosphere [online serial] 8(6):e01846.

Smith, J. J. 1990. The effects of sandbar formation and inflows on aquatic habitat and fish utilization in Pescadero, San Gregorio, Waddell and Pomponio Creek estuary/lagoon systems, 1985–1989. San Jose State University, San Jose, California.

Sommer, T., B. Harrell, M. Nobriga, R. Brown, P. Moyle, W. Kimmerer, and L. Schemel. 2001. California's Yolo Bypass: evidence that flood control can be compatible with fisheries, wetlands, wildlife, and agriculture. Fisheries 26(8):6–16.

Sonke, C. L. 2020. Outmigrant trapping of juvenile Chinook Salmon in the lower Tuolumne River, 2019. Submitted to the Turlock and Modesto Irrigation Districts by FISHBIO, Oakdale, California.

Soulé, M. E. 1987. Viable populations for conservation. Cambridge University Press, Cambridge, UK.

Stanley, C. E., R. J. Bottaro, and L. A. Earley. 2020. Monitoring adult Chinook Salmon, Rainbow Trout, and steelhead in Battle Creek, California, from March through November 2019. U.S. Fish and Wildlife Service, Red Bluff Fish and Wildlife Office, Red Bluff, California.

Steenweg, R., M. Hebblewhite, D. Gummer, B. Low, and B. Hunt. 2016. Assessing potential habitat and carrying capacity for reintroduction of plains bison (*Bison bison bison*) in Banff National Park. PLOS (Public Library of Science) ONE [online serial] 11(2):e0150065.

Stillwater Sciences. 2012. Modeling habitat capacity and population productivity for spring-run Chinook Salmon and steelhead in the upper Yuba River watershed. Prepared for the National Marine Fisheries Service, Santa Rosa, California, by Stillwater Sciences, Berkeley, California.

Sturrock, A. M., S. M. Carlson, J. D. Wikert, T. Heyne, S. Nussle, J. E. Merz, H. J. W. Sturrock, and R. C. Johnson. 2020. Unnatural selection of salmon life histories in a modified riverscape. Global Change Biology 26:1235–1247.

Sturrock, A. M., J. D. Wikert, T. Heyne, C. Mesick, A. E. Hubbard, T. M. Hinkelman, P. K. Weber, G. E. Whitman, J. J. Glessner, and R. C. Johnson. 2015. Reconstructing the migratory behavior and long-term survivorship of juvenile Chinook Salmon under contrasting hydrologic regimes. PLOS (Public Library of Science) ONE [online serial] 10(5):e0122380.

Taylor, J. E. I. 1999. Making salmon: an environmental history of the Northwest fisheries crisis. University of Washington Press, Seattle.

Taylor, T. N., B. K. Cross, and B. C. Moore. 2020. Modeling Brook Trout carrying capacity in Owhi Lake, Washington, using bioenergetics. North American Journal of Fisheries Management 40:84–104.

Thompson, N. F., E. C. Anderson, A. J. Clemento, M. A. Campbell, D. E. Pearse, J. W. Hearsey, A. P. Kinziger, and J. C. Garza. 2020. A complex phenotype in salmon controlled by a simple change in migratory timing. Science 370:609–613.

Tonina, D., J. A. McKean, R. M. Benjankar, C. W. Wright, J. R. Goode, Q. Chen, and M. R. Edmondson. 2019. Mapping river

bathymetries: evaluating topobathymetric LiDAR survey. Earth Surface Processes and Landforms 44:507–520.

Torgersen, C. E., D. M. Price, H. W. Li, and B. A. McIntosh. 1999. Multiscale thermal refugia and stream habitat associations of Chinook Salmon in northeastern Oregon. Ecological Applications 9:301–319.

USACE (U.S. Army Corps of Engineers). 2016. HEC-RAS River Analysis System: hydraulic reference manual. USACE, Davis, California.

Ver Hoef, J. M., E. E. Peterson, D. Clifford, and R. Shah. 2014. SSN: an R package for spatial statistical modeling on stream networks. Journal of Statistical Software [online serial] 56(3).

Verhille, C. E., K. K. English, D. E. Cocherell, A. P. Farrell, and N. A. Fangue. 2016. High thermal tolerance of a Rainbow Trout population near its southern range limit suggests local thermal adjustment. Conservation Physiology 4(1):cow057.

Ward, P. D., T. R. McReynolds, and C. E. Garman. 2004. Butte Creek spring-run Chinook Salmon, *Oncorhynchus tshawytscha* pre-spawn mortality evaluation 2003. California Department of Fish and Game, Inland Fisheries, Administrative Report 2004-5, Rancho Cordova.

Wheaton, J. M., N. Bouwes, P. McHugh, C. Saunders, S. Bangen, P. Bailey, M. Nahorniak, E. Wall, and C. Jordon. 2018. Upscaling site-scale ecohydraulic models to inform salmonid population-level life cycle modeling and restoration actions—lessons from the Columbia River basin. Earth Surface Processes and Landforms 43:21–44.

Wilkins, B. C., and N. P. Snyder. 2011. Geomorphic comparison of two Atlantic coastal rivers: toward an understanding of physical controls on Atlantic Salmon habitat. River Research and Applications 27:135–156.

Williams, J. G. 1996. Lost in space: minimum confidence intervals for idealized PHABSIM studies. Transactions of the American Fisheries Society 125:458–465.

Williams, J. G. 2010. Sampling for environmental flow assessments. Fisheries 35:434–443.

Williams, J. G. 2012. Juvenile Chinook Salmon (*Oncorhynchus tshawytscha*) in and around the San Francisco Estuary. San Francisco Estuary and Watershed Science [online serial] 10(3):article 2.

Williams, T. H., B. C. Spence, D. A. Boughton, R. C. Johnson, L. G. Crozier, N. J. Mantua, M. R. O'Farrell, and S. T. Lindley. 2016. Viability assessment for Pacific salmon and steelhead listed under the Endangered Species Act: Southwest. NOAA Technical Memorandum NMFS-SWFSC-564.

Wood, S. N. 2006. Generalized additive models: an introduction with R. Chapman and Hall/CRC Press, Boca Raton, Florida.

Wyrick, J. R., A. E. Senter, and G. B. Pasternack. 2014. Revealing the natural complexity of fluvial morphology through 2D hydrodynamic delineation of river landforms. Geomorphology 210:14–22.

Yoshiyama, R. M., F. W. Fisher, and P. B. Moyle. 1998. Historical abundance and decline of Chinook Salmon in the Central Valley region of California. North American Journal of Fisheries Management 18:487–521.

Yoshiyama, R. M., E. R. Gerstung, F. W. Fisher, and P. B. Moyle. 2001. Historical and present distribution of Chinook Salmon in the Central Valley drainage of California. California Department of Fish and Game Fish Bulletin 179:72–176.

Zeug, S. C., K. Sellheim, J. Melgo, and J. E. Merz. 2020. Spatial variation of juvenile Chinook Salmon (*Oncorhynchus tshawytscha*) survival in a modified California river. Environmental Biology of Fishes 103:465–479.

Zeug, S. C., K. Sellheim, C. Watry, J. D. Wikert, and J. Merz. 2014. Response of juvenile Chinook Salmon to managed flow: lessons learned from a population at the southern extent of their range in North America. Fisheries Management and Ecology 21:155–168.

Zeug, S. C., J. Wiesenfeld, K. Sellheim, A. Brodsky, and J. E. Merz. 2019. Assessment of juvenile Chinook Salmon rearing habitat potential prior to species reintroduction. North American Journal of Fisheries Management 39:762–777.

SUPPORTING INFORMATION

Additional supplemental material may be found online in the Supporting Information section at the end of the article.